Marine Geology 423 (2020) 106137

Contents lists available at ScienceDirect

Marine Geology

journal homepage: www.elsevier.com/locate/margo

Fate of Ayeyarwady and Thanlwin Rivers Sediments in the Andaman Sea and Bay of Bengal

J. Paul Liu[a,*], Steven A. Kuehl[b], Austin C. Pierce[a], Joshua Williams[b], Neal E. Blair[c], Courtney Harris[b], Day Wa Aung[d], Yin Yin Aye[e]

[a] Department of Marine, Earth, and Atmospheric Sciences, North Carolina State University, Raleigh, NC, USA
[b] Virginia Institute of Marine Science, William & Mary, Gloucester Point, VA, USA
[c] Department of Earth and Planetary Sciences, Northwestern University, Evanston, IL, USA
[d] Department of Geology, University of Yangon, Yangon, Myanmar
[e] Department of Geology, Mawlamyine University, Mawlamyine, Myanmar

ARTICLE INFO

Editor: Edward Anthony

Keywords:
Ayeyarwady
Andaman Sea
Gulf of Martaban
Sediment transport
Subaqueous Delta
Clinoform
Bay of Bengal

ABSTRACT

Collectively, the modern Ayeyarwady (Irrawaddy) and Thanlwin (Salween) rivers deliver > 600 Mt/yr of sediment to the sea. To understand the fate of Ayeyarwady and Thanlwin river-derived sediments to the sea, we conducted a 14-day geophysical and geological survey in the northern Andaman Sea and eastern Bay of Bengal in December 2017. Overall, ~1500-km of high-resolution Chirp-sonar profiles and 30 sediment cores from the shelf were acquired. This paper presents the results of the processed high-resolution profiles together with sediment analyses. Our findings indicate: 1) There is little modern sediment accumulating on the shelf immediately off the Ayeyarwady River mouths. In contrast, a major mud wedge with a distal depocenter, up to 60 m in thickness, has been deposited seaward in the Gulf of Martaban, extending to ~130 m water depth into the Martaban Depression. Further, 2) There is no evidence showing that modern sediment has accumulated or is transported into the Martaban Canyon; 3) There is a mud drape/blanket wrapping around the narrow western Myanmar Shelf in the eastern Bay of Bengal. The thickness of the mud deposit is up to 20 m nearshore and gradually thins to the slope at −300 m water depth, and likely escapes into the deep Andaman Trench; 4) The estimated total amount of Holocene sediments deposited offshore is ~1290 × 10^9 tons. If we assume this has mainly accumulated since the middle Holocene highstand (~6000 yr BP) like other major deltas, the historical annual mean depositional flux on the shelf would be 215 Mt/yr, which is equivalent to ~35% of the modern Ayeyarwady-Thanlwin rivers derived sediments; 5) Unlike other large river systems in Asia, such as the Yangtze and Mekong, this study indicates a bi-directional transport and depositional pattern controlled by the local currents that are influenced by tides, and seasonally varying monsoons winds and waves. Organic carbon biomarkers and isotope compositions show a gradual changing pattern with the along-shelf transport from the river to the Gulf of Martaban in the east and to the Bay of Bengal in the west.

1. Introduction

The uplifted Himalayan mountains and Tibetan Plateau in central Asia have developed > 10 major river systems — the Yellow, Yangtze, Pearl and Red rivers in the east side; the Mekong, Salween, Irrawaddy, and Ganges- Brahmaputra (G-B) rivers in the south; and the Indus River in the west (Fig. 1). Asian and Oceania rivers together have contributed > 70% of the historical global riverine sediments to the sea (Milliman and Farnsworth, 2011). The above-mentioned rivers alone discharge nearly 4 × 10^9 tons, approximately 25% of the global sediment flux to the sea (Liu et al., 2009). Consequently, this sediment flux results in many large deltas forming along the Asian ocean margins. Of the eleven major world deltas with an area size of > 20,000 km^2, six originate from the Himalaya mountain ranges.

Over the last 30 years, many surveys have been conducted on Asian continental shelves immediately offshore of these river mouths and adjacent margins to better understand the nature of the fate of Himalayan riverine sediments to the sea. These studies include, but are not limited to: the Yellow (Alexander et al., 1991; Liu et al., 2004), Yangtze (Liu et al., 2006, 2007; Xu et al., 2012), Pearl (Ge et al., 2014; Gao et al., 2015), Red (van Maren, 2007), Mekong (Xue et al., 2010; DeMaster et al., 2017; Liu et al., 2017), Ganges-Brahmaputra (Kuehl

* Corresponding author.
E-mail address: jpliu@ncsu.edu (J.P. Liu).

https://doi.org/10.1016/j.margeo.2020.106137
Received 7 September 2019; Received in revised form 24 January 2020; Accepted 27 January 2020
Available online 01 February 2020

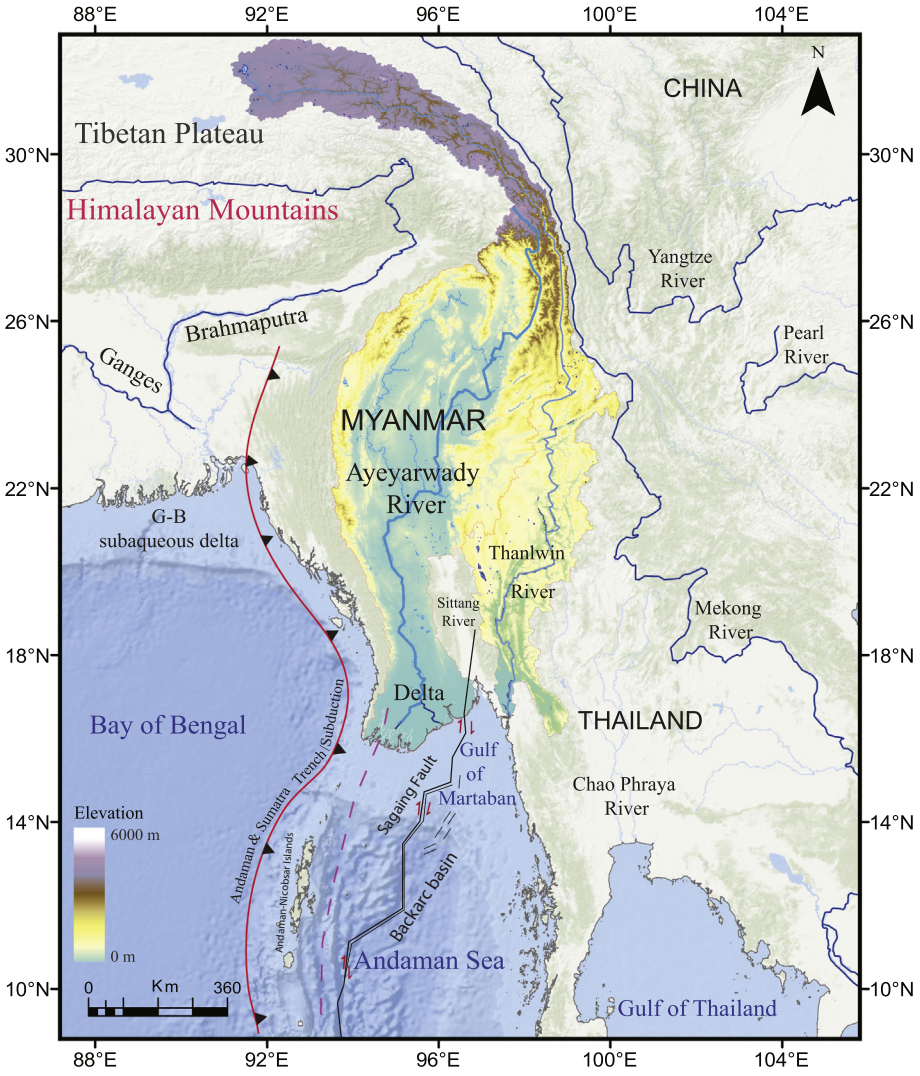

Fig. 1. Location map showing the Ayeyarwady and Thanlwin river basins and deltas; Tectonic map shows the Andaman and Sumatra Trench and Subduction in the Bay of Bengal, and spreading and sliding faults in the backarc basin across the Andaman Sea and Gulf of Martaban (based on Rodolfo, 1969 and Curray, 2005).

et al., 1997; Goodbred and Kuehl, 2000), Indus (Giosan et al., 2006; Clift et al., 2014). These studies revealed clear distribution patterns among the subaqueous deltas on the shelves, and provided a basic understanding of sediment transport dynamics and the mechanisms surrounding clinoform formation (see review papers of Walsh and Nittrouer, 2009; Liu et al., 2009; Patruno et al., 2015, Hanebuth et al., 2015).

The Ayeyarwady (Irrawaddy) and Thanlwin (Salween) rivers flow southward from the Himalayan mountains, discharging directly into the Andaman Sea. Collectively these two rivers discharge > 600 × 10^6 tons (or 600 Mt) of sediment annually to the sea (Furuichi et al., 2009; Robinson et al., 2007). A preliminary study of particulate and dissolved organic carbon (OC) transport in the Ayeyarwady and Thanlwin rivers indicates this combined river system transports 5.7–8.8 Mt./yr of organic carbon, suggesting that it may be the second largest point source of organic carbon to the global ocean after the Amazon (Bird et al., 2008). The Ayeyarwady and Thanlwin rivers drain ~ 0.5% of global continental area but deliver about 3.3% of the global silicate-derived dissolved Ca + Mg fluxes and 2.6% of the global Sr riverine fluxes to the oceans (Chapman et al., 2015). Some geological surveys and geochemical studies have been conducted in the Andaman Sea, but mainly focused on surficial sediments, such as Ramaswamy et al., 2004, 2008; Rao et al., 2005; Damodararao et al., 2016, etc. Until our most recent survey (i.e. Kuehl et al., 2019), very little was known about the distribution and accumulation of Holocene subsurface sediments.

Among the world major rivers, the Ayeyarwady and the Thanlwin are presently considered the last remaining long free-flowing large rivers in Asia outside of the Arctic (Grill et al., 2019). Tectonic processes have created an environment in which the Ayeyarwady delta regularly experiences significant flooding and is highlighted as one of the deltas “in peril” due to low elevation, subsidence, and global mean sea-level rise (Syvitski et al., 2009). With near future plans to dam the Ayeyarwady River and reduce sediment input to a system already at equilibrium, the need for comprehensive understanding of the distribution of the river's Holocene subaqueous delta and sediment dispersal patterns is clear. At present, the internal structure and sequence stratigraphy of its underwater clinoform and sediment transport mechanisms have not been studied.

To understand the fates of the Ayeyarwady and Thanlwin rivers derived sediments once they reach the sea, we conducted a 14-day geological and geophysical survey on the shelf of the northern Andaman Sea and eastern Bay of Bengal in December 2017. Recently, we reported on results from the sediment core analyses and CTD casts, along with some representative Chirp profiles (Kuehl et al., 2019). Supplementing that data set, here we present detailed analyses of the newly acquired high-resolution Chirp sonar data from the Andaman Sea and Bay of Bengal together with organic carbon biomarkers and isotope compositions derived from the geochemical analysis. These new results

provide a more complete understanding of the subaqueous delta distribution and Holocene sediment budget, as well as the clinoform's internal structures, and the roles that tectonic and oceanographic processes played in controlling sediment transport.

2. Background

The Ayeyarwady (Irrawaddy) and Thanlwin (Salween) rivers both traverse > 2000 km, spanning from the Himalayan mountains in the north, to the Gulf of Martaban of the Andaman Sea in the south (Fig. 1). The catchment areas of the Ayeyarwady and Thanlwin rivers are about 410×10^3 km^2 and 324×10^3 km^2, respectively. In Myanmar alone, these two rivers together cover > 560×10^3 km^2, equivalent to 83% of the country (Fig. 1). The Ayeyarwady River discharges > 430 km^3 of fresh water annually. For a global comparison it is ranked as the 5th largest river in terms of suspended sediment load (~360 Mt) and the 4th highest total dissolved load (Rao et al., 2005; Furuichi et al., 2009; Robinson et al., 2007). Together with the Thanlwin, the annual sediment load from these two rivers is estimated to be 600 Mt. (Robinson et al., 2007).

Seasonal monsoons impact the Ayeryarwady – Thanlwin systems. During the southwest monsoon (roughly May – October), winds are strong and from the southwest, and southern Myanmar receives heavy precipitation, with some areas exceeding 5 m/yr (Damodararao et al., 2016). In contrast, during the northeast monsoon season (October – February), conditions are dryer and winds are weaker and from the northeast.

2.1. The Ayeyarwady Delta

The Ayeyarwady River discharges southward and has gradually infilled a back-arc and strike-slip basin since the Cenozoic (Curray, 2005) (Figs. 1, 2). During the Holocene, sediments from the Ayeyarwady River have accumulated, forming a large triangle-shaped alluvial delta plain (35,000 km^2) between the Indo-Burman Range to the west and Bago-Yoma Range to the east (Fig. 2). Over the last 6–7 ka, the Ayeyarwady delta has prograded around 270 km from its apex at Henzada, to its present coastal zone in the Northern Andaman Sea (Giosan et al., 2018). This indicates that the long-term averaged progradation rate is around 40 m/yr, a rate comparable to other Asian major deltas, like the Mekong (Ta et al., 2001; Liu et al., 2017). However, recent studies suggest that the coastline of this delta has been largely stable for the last 150 years, raising the possibility of shoreline erosion in the coming years if sediment supply is reduced due to natural or anthropogenic alteration such as increased major storm systems and damming (Hedley et al., 2010; Anthony et al., 2019). For instance, following Cyclone Nargis in May of 2008, the Ayeyarwady shoreline showed a mean retreat of 47 m (Besset et al., 2017).

The Ayeyarwady Delta is classified as a mud-silt, tide-dominated system with a mean tidal range of 4.2 m and tidal influences that extend almost 300 km upstream to the apex of the delta at Henzada (Fig. 2) (Hedley et al., 2010). This alluvial delta plain spans nearly 300 km in the Gulf of Martaban, from its distributary channel of Pathein River in the west to the Yangon river in the east (Fig. 2). Due to the extensive lowlands and high-frequency of tropical cyclones, the Ayeyarwady River Delta is often inundated. For example, Cyclone Nargis in 2008 inundated an area up to 15,000 km^2 with 6 m of floodwater above sea level (Syvitski et al., 2009), and caused > 138,000 fatalities (Fritz et al., 2009).

2.2. The Gulf of Martaban and Andaman Sea

The Andaman Sea is a marginal sea in the eastern Indian Ocean with an area of 800,000 km^2. The Andaman Sea is partitioned from the Indian Ocean by the Bay of Bengal to its west and by the Andaman and the Nicobar Islands in the southwest (Rodolfo, 1969, 1975). It is bounded to the north by the Ayeyarwady River delta, to the east by peninsular Myanmar, Thailand and Malaysia (Figs. 1, 2). Tectonically, the Andaman Sea is an active backarc basin lying above and behind the Sunda-Sumatra subduction zone. The backarc extension and strike-slip motion formed a deep backarc basin (up to 3000 m) in the central part, and N-S Sagaing Fault extending northward from the deep central basin to the delta plain (Curray, 2005) (Fig. 1).

Due to the long-term accumulation of high sediment fluxes from the Ayeyarwady and Thanlwin rivers since the late Miocene, the northern part of the Andaman Sea (aka, Gulf of Martaban) is much shallower (Morley, 2013) (Figs. 2, 3). Offshore, the Ayeyarwady delta has formed a broad continental shelf, up to 170 km wide, to the 200-m isobath (Rodolfo, 1969). The most prominent bathymetric feature on the Ayeyarwady continental shelf is the 120-km-wide Martaban Depression (Figs. 2, 4) (Ramaswamy and Rao, 2014). This bathymetric depression is located on the outer shelf between the Sagaing Fault system and Malay continental margin, extending 100 km offshore from 50 m to 150 m water depths. Farther offshore, at around 14°N and 96°E, this depression opens into a 500-m-deep V-shape Martaban Canyon, that connects to the 2000-m-deep backarc basin and has been proposed to be an offshelf sediment transport conduit (Rao et al., 2005).

Previous studies have indicated that the continental shelf of Myanmar is strongly controlled by seasonal monsoon winds, waves, tides and coastal currents (Rodolfo, 1969; Ramaswamy et al., 2004). The southwest monsoon (May –September) is the rainy season, a time when the country receives 90% of its annual precipitation and wind speeds average 30 km/h. The overall surface circulation is cyclonic, moving from the Bay of Bengal eastward into the Gulf of Martaban and Andaman Sea, and then turning southward along the Myanmar-Thailand Peninsula (Fig. 3) (Rodolfo, 1969; Ramaswamy and Rao, 2014). This dynamic causes a large amount of low-saline water (< 20‰) to gather in the Gulf of Martaban. During the northeast monsoon (December–February), northeasterly winds blow 15–29 km/h, encouraging overall westward surface flow from the Andaman Sea into the Bay of Bengal (Rodolfo, 1969).

The Gulf of Martaban is a tide-dominated bay with variable tidal ranges. The dominant tide in this area is semi-diurnal with M2 and S2 components (Sindhu and Unnikrishnan, 2013). Tidal ranges in the northern reaches of the Gulf are ~4 m and increase along the eastern and western coasts of the Gulf (Sindhu and Unnikrishnan, 2013; Ramaswamy et al., 2004). Along the Ayeyarwady Delta, the highest tidal range of 7 m is found at Elephant Point, while the Ayeyarwady River mouth, is characterized as meso-tidal with a range between 2 and 4 m (Ramaswamy et al., 2004). The Ayeyarwady Delta is affected by waves of moderate fetch generated by southwesterly winds with a mean wave height of up to 2 m. The wave height normally reaches its peak during the summer southwest monsoon season, and diminishes during the winter northeast monsoon (Besset et al., 2017).

2.3. Offshore Sediment Accumulation

Due to the high sediment discharge from adjacent rivers, the prevailing monsoonal winds, strong wave and tidal currents, and shallow water depth, the Gulf Martaban experiences suspended sediment concentrations up to 500 mg/l, making it one of the world's largest high turbidity zones, (Ramaswamy et al., 2004). Remote sensing data reveals a near homogenous surface suspended sediment concentration (SSC) turbid water covering the entire Gulf of Martaban during the northeast monsoon season. Though > 80% of the annual sediment flux is discharged during the southwest monsoon season (Rodolfo, 1969), a relatively low and sparse SSC area was observed in the Gulf of Martaban during southwest monsoon conditions (Matamin Abd et al., 2015). The Gulf of Martaban shows an extremely high SSC during the passing of tropical cyclones; for instance, the SSC was up to 50% above average during the passage of Tropical Cyclone Nargis in 2008 (Besset et al., 2017). In addition to the seasonal variations, the distribution of the

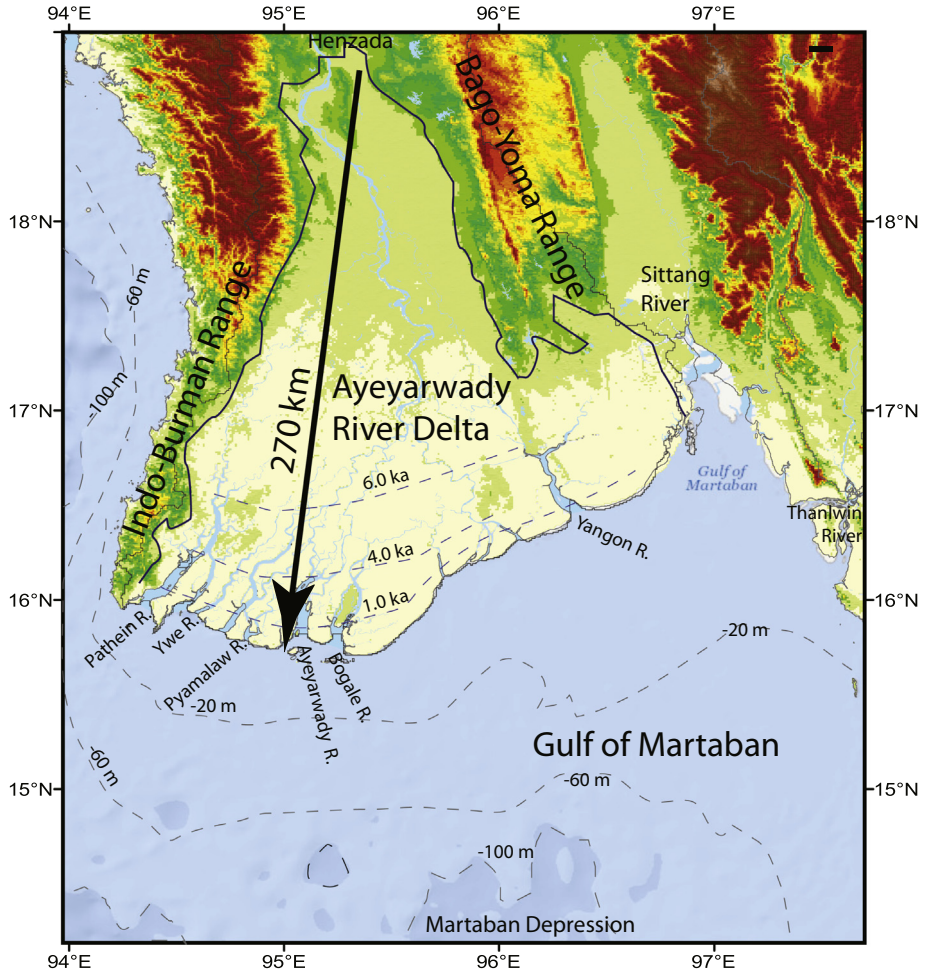

Fig. 2. Distribution and progradation of the Ayeyarwady River Delta in the past 6–7 ka and its main distributary channels. The estimated historical shoreline positions are derived from Giosan et al. (2018). On average, in the past 7 ka, the delta has prograded at a rate of 40 m/yr.

turbid water also changes with the tidal cycles: i.e. during the spring tide, when the tidal range is around 6.6 m, the turbid water covers > 45,000 km^2; during neap tide, with tidal range of 3.0 m, the highly turbid water coverage drops to 15,000 km^2. The edge of the highly turbid zone migrates by nearly 150 km across the gulf in-sync with every tidal cycle (Rao et al., 2005).

Previous study of 110 surface sediment samples collected from the Ayeyarwady continental shelf found 1) an extensive near-shore mud belt covering an area of 45,000 km^2 in the Gulf of Martaban and adjacent inner shelf; 2) no predominant mud accumulation on the shelf offshore of the Ayeyarwady River Mouths; 3) relict sand dominating the outer shelf, and 4) mixed sediment with relict sands and modern mud in the Martaban Canyon (Rao et al., 2005). Furthermore, Ramaswamy and Rao (2014) inferred that the Martaban mud belt and high turbid waters extend partly into the Martaban Canyon where strong tidal forces, and gravity flows (possibly hyperpycnal) help transport sediment directly into the deep Andaman Sea. They speculated that the Martaban Canyon might act as a deep water conduit for sediments to the deep basin. Recently, based primarily on seabed and water column samples and data collected during our 2017 cruise, we (Kuehl et al., 2019) show century-scale accumulation rates up to ~10 cm per year in the central Gulf of Martaban, and the presence of extensive fluid mud and deep seabed mixing-reoxidation driven by tides in shallower areas of the Gulf. Elsewhere on muddy portions of the shelf, accumulation rates are typically ~1 cm/yr. A conceptual model was proposed (Kuehl et al., 2019), highlighting the importance of tides, and seasonal monsoonal variations in winds, waves and circulation patterns in controlling the dispersal of the river's sediment along and across the gulf and shelf.

3. Data and methods

3.1. Field data collection

A 14-day research cruise was conducted in the study area using a local vessel (*Sea Princess*) in December 2017 by a joint team of scientists from Mawlamyine University, North Carolina State University, Virginia Institute of Marine Science, and Yangon University. More than 1500-km high-resolution Chirp sonar data were acquired from the Andaman Sea and Bay of Bengal (Fig. 4). Thirty sediment cores were collected using a 3-m long Kasten corer, and some stations were duplicated with 1.5-m long gravity or box corers (Fig. 4, Table 1). The Chirp sonar data was collected using the EdgeTech 424 and 0512i subbottom profiling systems, with a frequency of 4–16 kHz or 0.5–8.0 kHz, respectively. All seismic data were saved and backed up onboard digitally using the native EdgeTech JSF data format. All kasten and box cores were sampled onboard. Gravity cores were capped and sealed for further analyses in the lab. Some surface samples were frozen immediately onboard for organic geochemical analyses.

3.2. Chirp data analyses

All seismic and navigation data were post-processed using the EdgeTech Discover Sub-bottom software (Version 4.09). An acoustic velocity of 1500 m/s was used to calculate water depth and sediment

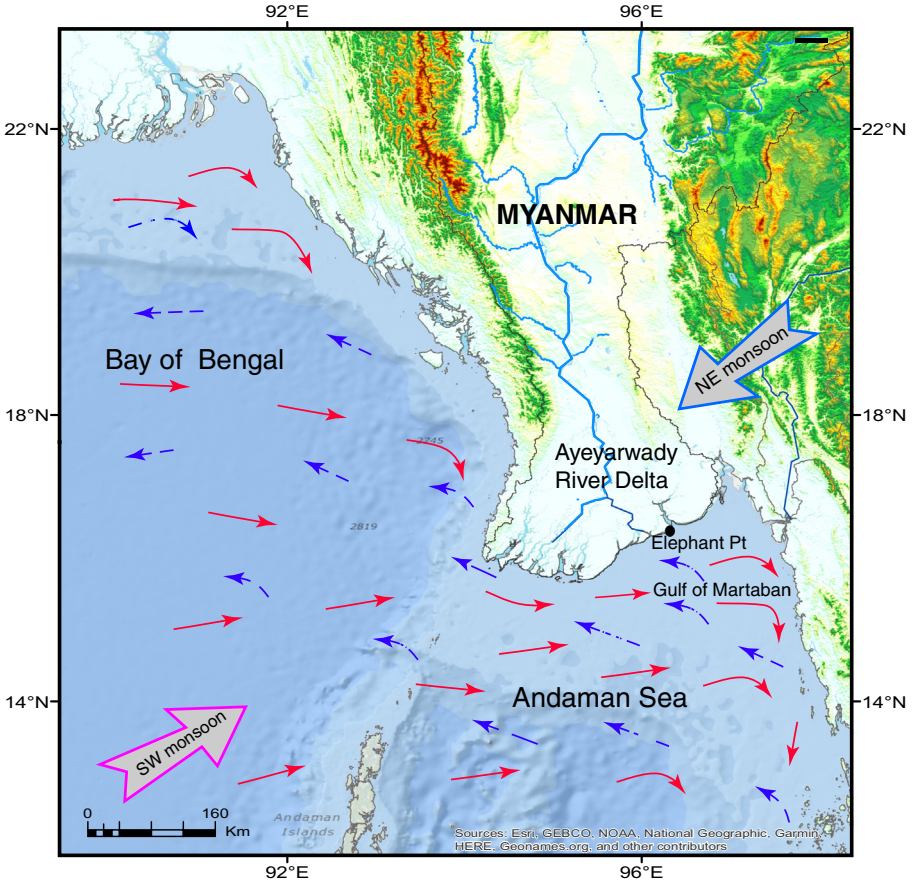

Fig. 3. General surface circulation patterns during the northeast (winter) and southwest (summer) monsoons (from Rodolfo, 1969, 1975). Overall, during the winter season, surface currents flow from the Andaman Sea to the Bay of Bengal (blue arrows), during the summer season, surface currents flow from the Bay of Bengal into the Andaman Sea (red arrows). (For interpretation of the references to colour in this figure legend, the reader is referred to the web version of this article.).

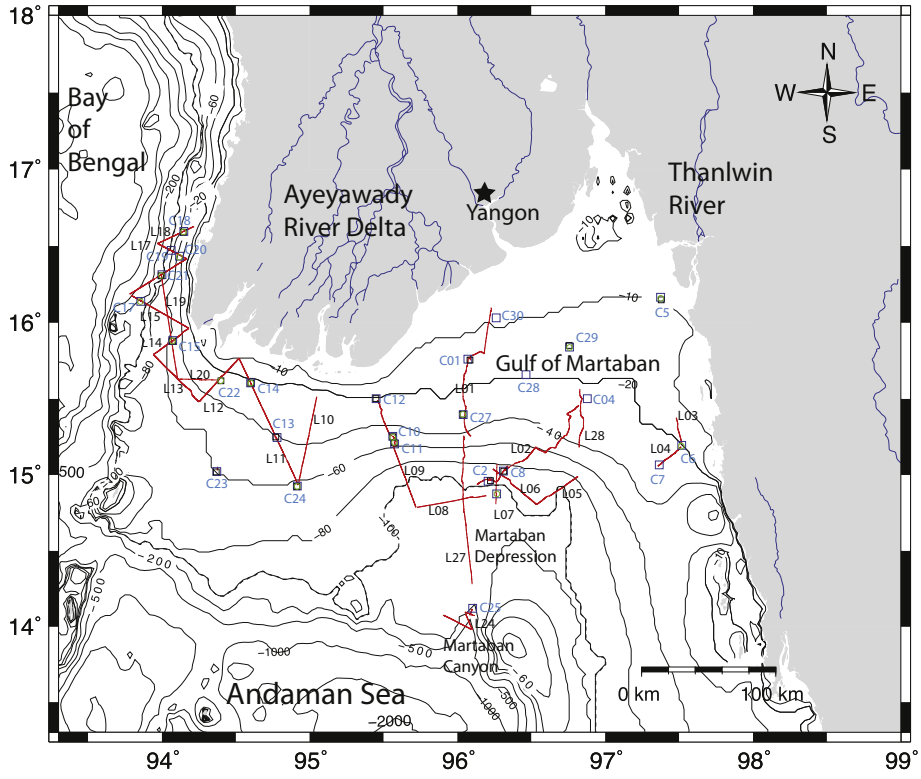

Fig. 4. Location map of the Chirp sonar seismic tracklines and coring stations from the 2017 research cruise (e.g. L27 is the Chirp profile number, C12 is the coring station number).

Table 1
Sediment core locations, water depths, ^{210}Pb-derived accumulation rates, C/N, δ^{13}C, and the sums of lignin phenols (normalized), and lignin vanillyl acid/aldehyde ratios.[a]

Core stations	Length (cm)	Water depth (m)	Latitude	Longitude	^{210}Pb-derived accumulation rate with range (cm/yr)[a]	δ^{13}C (‰)	C/N (wt)	ΣLignin phenols (relative concentration)	Vanillyl phenol acid/aldehyde ratio
BC-KC 01	180	5	15°45.600′N	96°04.199′E	1.4–2.0 (1.7)				
BC-KC 02	280	75	14°57.476′N	96°12.403′E	6.8–9.4 (7.9)				
BC-KC 04	300+	21	15°30.041′N	96°52.721′E					
BC-KC 05	300+	15	16°09.918′N	97°22.420′E					
BC-KC 06	300+	25	15°11.643′N	97°31.013′E					
BC-KC 07	217	28	15°03.933′N	97°21.926′E	0.2–0.4 (0.3)				
BC-KC 08	300+	45	15°01.508′N	96°18.651′E	6.9–10.7 (8.4)				
BC-KC 09	300	125	14°52.495′N	96°15.864′E	3.5–4.0 (3.7)				
BC-KC 10	300+	35	15°15.178′N	95°33.725′E					
BC-KC 11	260	55	15°12.191′N	95°34.425′E	2.9–3.5 (3.2)				
BC-KC 12	65	10	15°30.044′N	95°26.971′E					
BC-KC 13	68	35	15°14.734′N	94°46.740′E	0.2–0.4 (0.3)				
BC-KC 14	100	20	15°36.250′N	94°35.993′E		−24.91	8.52	1.0000	0.3540
BC-KC 15	237	38	15°52.921′N	94°04.368′E					
BC-KC 16	S	13	15°57.715′N	94°11.016′E					
BC-KC 17	170	110	16°08.300′N	93°51.416′E					
BC-KC 18	253	53	16°35.738′N	94°08.888′E	0.9–1.1 (1.0)	−23.76	7.15	0.5324	0.4592
BC-KC 19	220	77	16°28.291′N	94°03.734′E					
BC-KC 20	15	45	16°26.023′N	94°07.132′E					
BC-KC 21	230	90	16°18.753′N	93°59.984′E	0.7–0.9 (0.8)	−23.55	7.80	0.5564	0.3833
BC-KC 23	90	50	15°01.288′N	94°22.287′E	0.4–0.6 (0.5)	−21.98	6.94	0.0730	3.2471
BC-KC 24	300+	58	14°55.558′N	94°54.966′E		−22.02	6.80	0.0751	1.6023
BC-KC 25	75	170	14°07.217′N	96°06.161′E	0.0				
BC-KC 27	246	20	15°23.779′N	96°02.303′E		−23.50	6.71	0.2046	0.7382
BC-KC 28	?	17	15°39.475′N	96°27.790′E					
BC-KC 29	300+	17	15°50.315′N	96°45.498′E	0.4	−23.83	6.95	0.2013	0.7757
BC-KC 30	?	8	16°01.812′N	96°15.689′E		−24.18	7.18	0.2165	0.6918

[a] From Kuehl et al. (2019).

thicknesses. All profiles were captured and saved as image files, processed further under image-editing software and ArcGIS, and then ultimately loaded into IVS Fledermaus to construct fence diagrams. Based on the data delineated from all Chirp sonar profiles, an overall subaqueous deltaic sediment distribution and isopach map was constructed. The sediment-thickness isopach data was imported into ArcGIS 10, and the distribution area, distance, and volume were calculated. In this study, we used a mean dry bulk density of 1.2 g/cm^3 to calculate the sediment mass of the subaqueous clinoform. To help explain the Chirp–sonar profiles and depositional processes, we also include our recently reported ^{210}Pb-derived accumulation rates (Kuehl et al., 2019) in the discussion.

3.3. Laboratory sediment analysis

To track the fate of river-derived sediment in the marine environment, we measured organic carbon (OC) contents (%C by dry weight), organic C to total N ratios (C/N on a per weight basis), ^{13}C/^{12}C ratios (δ^{13}C) and lignin phenols distributions. The C/N ratios, δ^{13}C values and lignin phenols provide proxies of terrestrial plant OC that are associated with fluvial inputs (e.g. Blair and Aller, 2012).

The frozen surface samples were dried and ground to a fine powder. Samples were treated with aqueous 2 N HCl for up to 48 h to remove carbonates. Carbonate removal was verified via transflectance FTIR (Cui et al., 2016) using a Bruker Tensor 37 FTIR [NIR/MIR] equipped with a Hyperion microscope and MCT detectors by monitoring an absorbance peak at 2513/cm.

The decarbonated sediment samples were analyzed for OC and total N concentrations and stable isotopic compositions using a Costech Elemental Analyzer-Conflo IV interface-Thermo Delta V Plus isotope ratio mass spectrometer (IRMS) combination. Isotopic compositions were related to international standards (VPDB, air) through calibrated laboratory reference materials (Leithold et al., 2013; Coplen, 2011) and reported using the δ^{13}C notation (Craig, 1953). POC and PN concentrations are reported as a percent of sediment dry weight.

Thermochemolysis using tetramethylammonium hydroxide (TMAH) as a methylating agent was used for the lignin phenol analysis. Approximately 50 mg of the sediment samples and 150 ul of TMAH (25% in methanol) were placed in a quartz boat as well as methyl-D3 pentadecanoic acid as an internal standard. The quartz boat with sample and reagent was at 300 °C for 30 s in a helium flow using a CDS 5200 pyroprobe. The volatile products were swept to a Trace Gas Chromatograph Ultra-DSQ II Mass spectrometer (Thermo Scientific) equipped with a TR-5MS column (30 m × 0.25 mm × 0.25 μm). The oven temperature was programmed from 50 to 330 °C with a ramp rate of 10 °C/min (Fournillier, 2016).

The methylated lignin phenols were identified based on their mass spectra compared to the NIST and user-created mass spectral libraries. Identifications were considered positive for compounds with RSI (reverse squared index) values of ≥800. Relative concentrations of the phenols were determined by normalizing TIC peak areas to that of the internal standard and the quantity of organic C in the sample. For a measure of relative lignin concentration, individual phenol values were totaled and the sums were normalized to that of the sample with the greatest quantity of lignin.

4. Results

High-resolution Chirp sonar profiles reveal an extensive mud wedge in the Gulf of Martaban, a limited subaqueous delta off the Ayeyarwady River mouth, and a mud drape in the Western Myanmar Shelf in the eastern Bay of Bengal. The organic geochemical parameters (%C, C/N, δ^{13}C, and lignin phenols) varied along gradients from the Ayeyarwady river mouth to the Bay of Bengal in the west and to the Gulf of Martaban in the east.

4.1. Chirp-sonar profiles revealed sediment distribution and stratigraphy

4.1.1. Area-1: the Gulf of Martaban mud deposit and clinoform

Eleven high-resolution Chirp-sonar profiles were collected in the

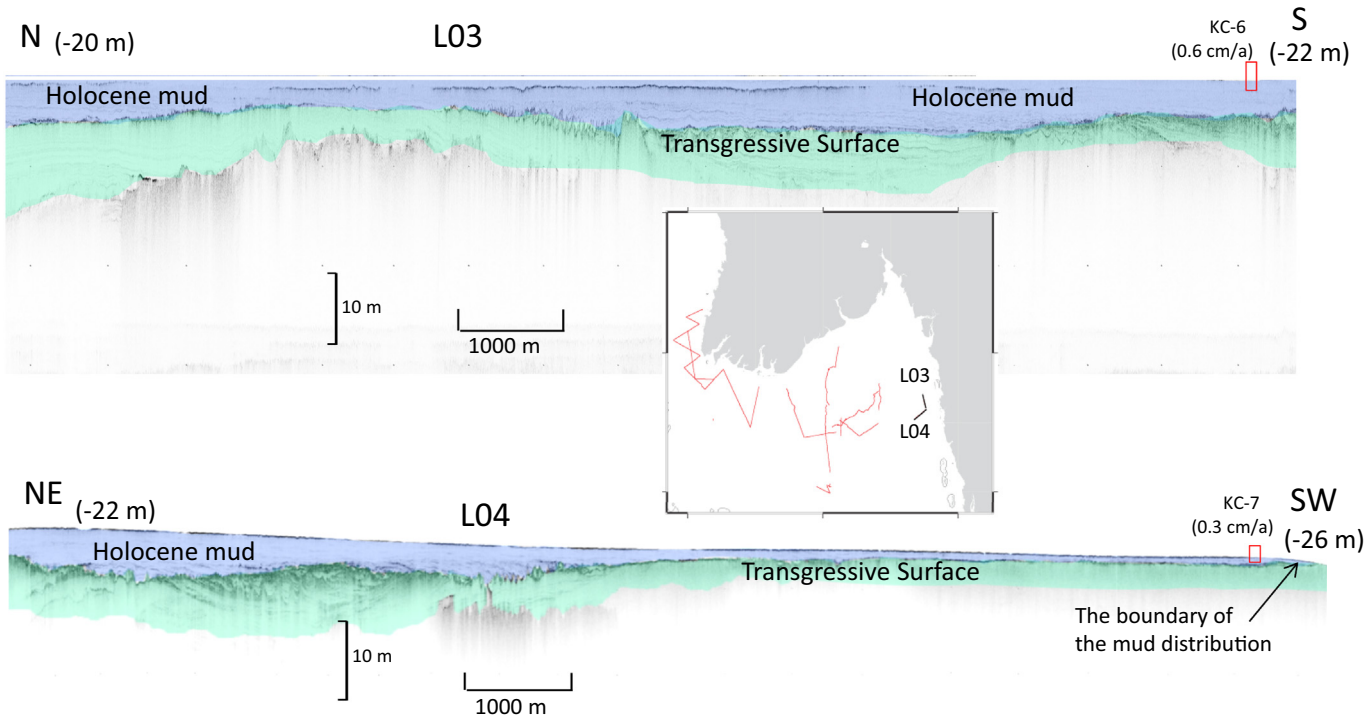

Fig. 5. Selected Chirp-sonar profiles (L03 and L04) in the eastern part of the study area, which shows the thickness of the Holocene mud deposits and the diminishing boundary of the mud distribution. The bluish color represents Holocene mud deposits, the greenish color represents the pre-Holocene deposits. The same coloration is used for all profiles discussed in this paper. (For interpretation of the references to colour in this figure legend, the reader is referred to the web version of this article.)

Gulf of Martaban between water depths of 10 to 130 m crossing the entire gulf to the shelf edge (Fig. 4). Lines 03 and 04 were located on the eastern side of our study area, where a 7–8 m thick mud deposit was found at the water depths of 20–22 m (Fig. 5). There is a rugged transgressive surface (TS) at the depth of 25 m separating the Holocene mud on the top and the underlying pre-Holocene strata. The pre-Holocene deposit was truncated by a strong transgressive process during the rapid sea-level rise. In Line 04, the Holocene mud gradually diminishes southwestward farther offshore at the water depth of 26 m (Fig. 5).

Lines 07 and 27 are located at the southwest edge of the Gulf Martaban (Figs. 4 and 6). They parallel to each other and run north to south between water depths 20 m and 140 m (Fig. 6). The high-resolution Chirp sonar profiles reveal a predominant mud wedge, up to 50 m thick, with a classic clinoform depositional features of topset, foreset and bottomset facies. Line 27 shows the topset at around 30 m water depth, steep foreset that ultimately pinches out at water depth around 90 m (Fig. 6). A 515-cm-long piston core StMY06 collected at the depth of 75 m was located at the seaward edge (bottomset) of this clinoform wedge on Line 27 (Ota et al., 2017). The mean ^{14}C-based accumulation rate for the upper portion (0–3.72 m) of the core was 1.2 cm/yr (Fig. 6), which is a little lower than the reported ^{210}Pb accumulation rate (Kuehl et al., 2019). Line 07's foreset also starts at water depth of 30 m, then dips down, and ends at a depth of 130 m. Seaward of these profiles, we found no evidence of modern mud accumulation on the outer shelf; instead, the predominant features were back-arc basin bookshelf faults and a rugged surface with high acoustic reflectivity (Fig. 6).

Line 02 intersects Line 07 at a near right-angle, and reveals a mud wedge that is up to 60 m thick (Fig. 7). Line 09 extends from the Ayeyarwady River mouths and is located along the western boundary of the Gulf Martaban and reveals a subaqueous deltaic mud deposit in water depths of 5 m to 110 m (Fig. 7). The thickness of the clinoform foreset in this area is up to 30 m. The rugged surface over the deeper part of Line 09 may reflect the crossing of the active Sagaing Fault (Figs.1 and 7).

4.1.2. Area-2: offshore off the Ayeyarwady River mouths

Different from the predominant mud wedge found in the Gulf of Martaban, Chirp sonar profiles (Lines 10, 11 and 12) on the shelf offshore of the Ayeyarwady River mouths, do not reveal an extensive clinoform deposit. Instead there appears to be no obvious modern mud accumulation on the middle and outer shelves directly off the Ayeyarwady River mouths (Figs. 8, 9). Line 10, off the eastern Ayeyarwady River delta, shows a very limited cross-shelf modern mud accumulation that is < 10 m in thickness, extends < 12 km, and is confined to water depths shallower than 20 m (Figs. 8, 9). Line 11 also shows a short and thin (< 10-m thick) clinoform deposit near the river mouths within water depths of 20 m (Fig. 8). Chirp sonar profiles outside of the nearshore mud deposit show only limited subsurface penetration (Fig. 9).

4.1.3. Area-3: western Myanmar shelf in the eastern Bay of Bengal

Chirp sonar profiles from the shelf, west of the Ayeyarwady Delta, in the eastern Bay of Bengal, indicate an up to 20-m thick mud deposit extending across the shelf and gradually thinning offshore to the outer shelf break and even to the upper slope (Fig. 10).

Due to the limitations of our vessel and tow cable, we were not able to map the seafloor at depths > 350 m. In contrast to the Gulf of Martaban, there appears to be no cross-shelf prograding subaqueous clinoform on the western Myanmar shelf, instead, this deposit exhibits a stratified “mud drape or blanket,” indicative of strong along-shelf transport and aggradation deposits.

4.1.4. Area-4: Martaban Depression and Canyon deposits

Chirp sonar profiles crossing the Martaban Canyon do not show any modern mud accumulation on the seafloor. The selected profiles, Lines 23 and 24, reveal a > 300–400 m deep V-shaped canyon without obvious mud deposition, progradation, or aggradation draping (Fig. 11). The sediment core KC-25 shows zero modern accumulation. The Chirp

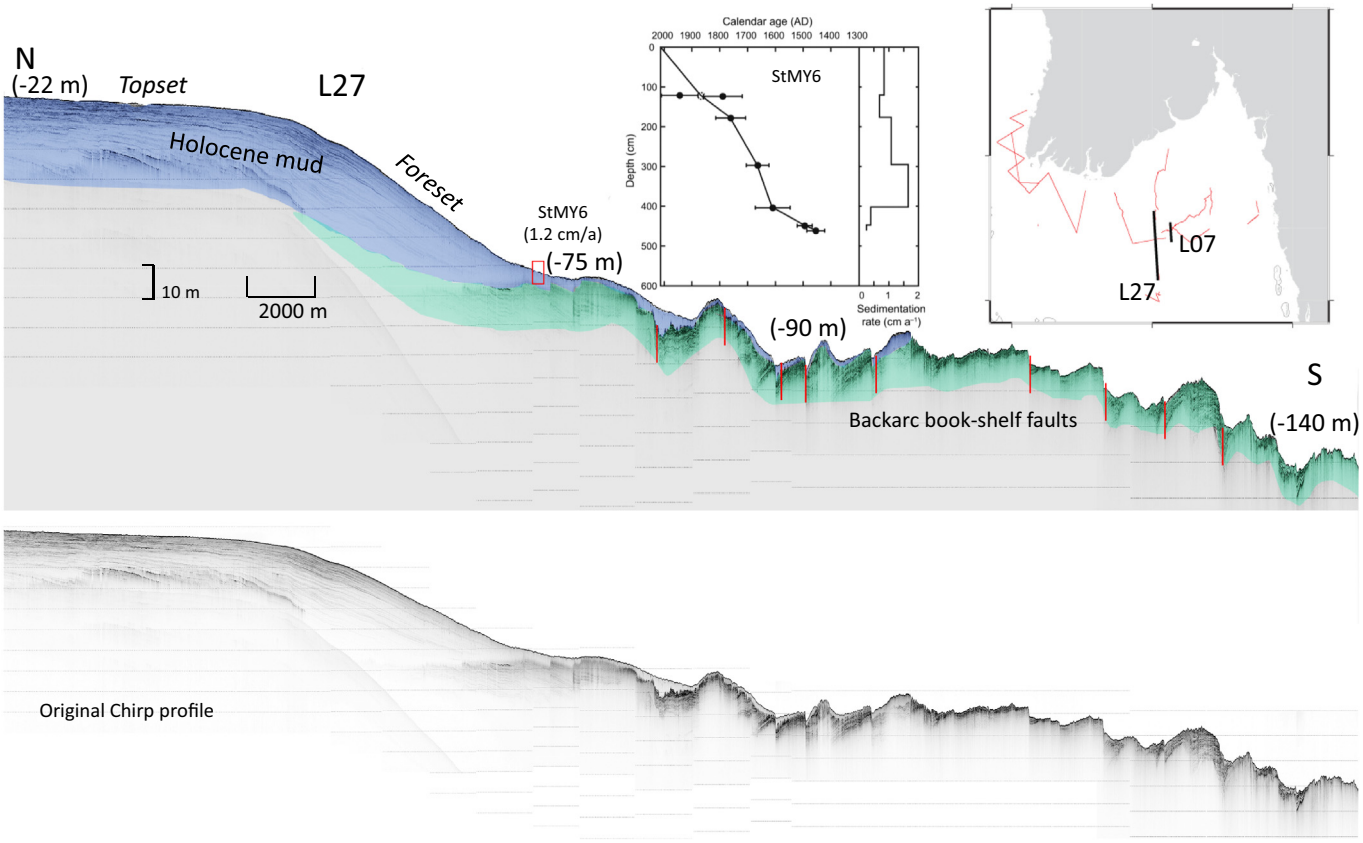

Fig. 6. Selected Chirp-sonar profiles (L07 and L27) in the middle part of the study area, which show the formation of a clinoform with rapid accumulation over the foreset. The profiles also indicate the Holocene muds stop at water depths of 90–130 m. There is no sign for further accumulation in the Martaban Depression, which is instead dominated by numerous book-shelf faults. The piston core StMY6's ages and sedimentation rates are from Ota et al. (2017).

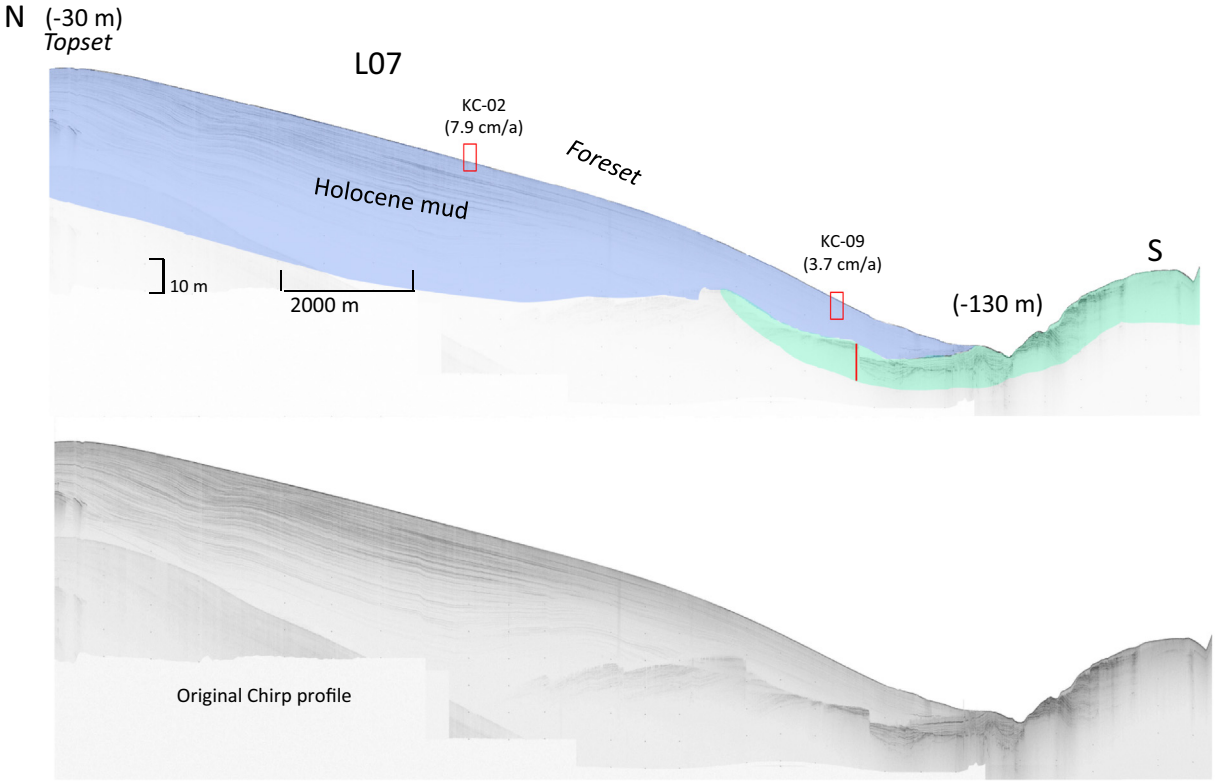

Fig. 6. (*continued*)

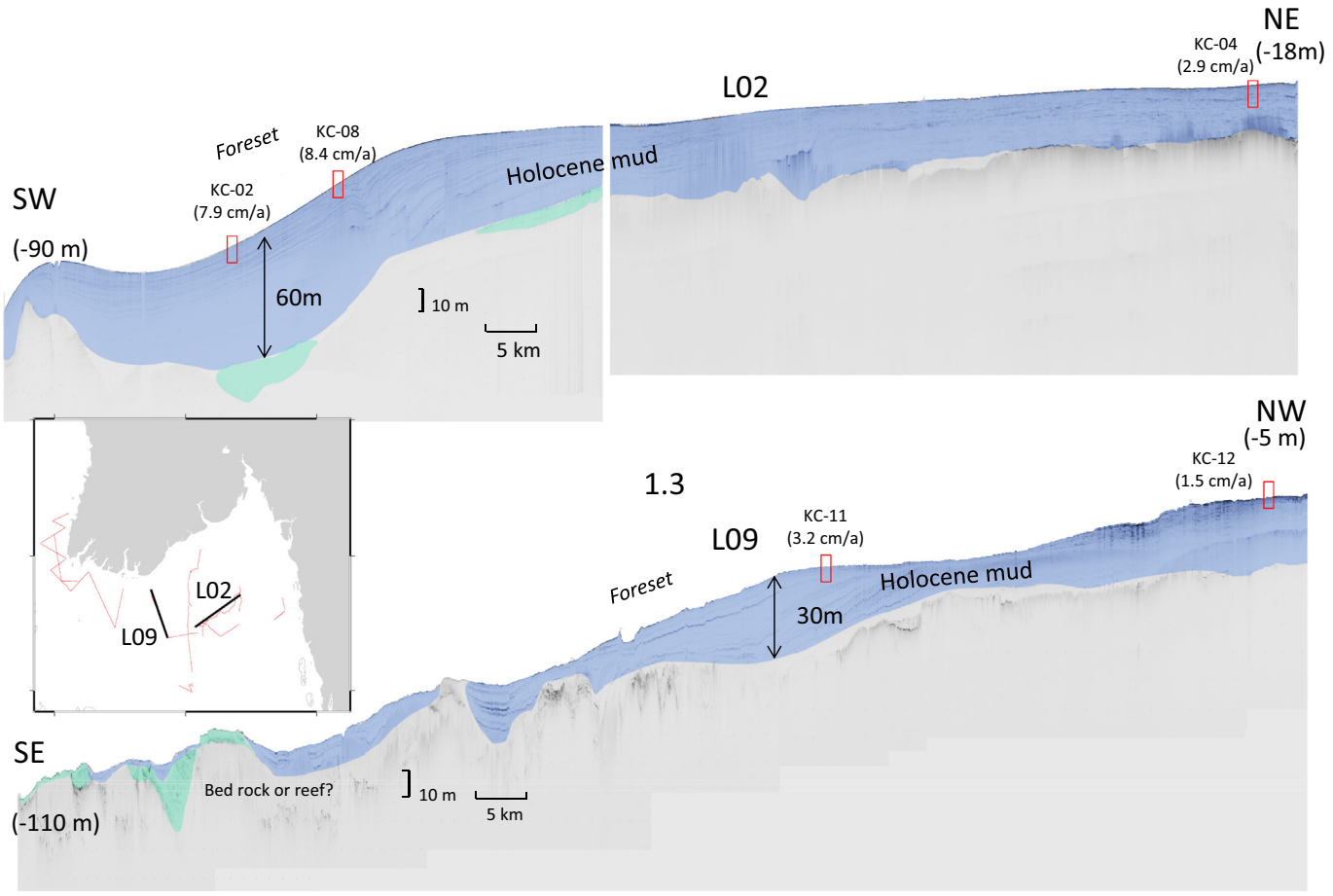

Fig. 7. Chirp-sonar profiles (L02 and L09) in the middle part of the study area, which show the formation of a clinoform with a rapid accumulation over the foreset.

profile collected between the canyon and the dominated mud wedge, between −140 and −90 m, provide no evidence of modern mud accumulation on the sea floor, as seen on southern end of the Line 27 profile (Fig. 6).

4.2. Sediment budget and mass balance

Based on available data of accumulation rates (Table 1) and Chirp sonar profiles (Figs. 6–11), conceptual maps of sedimentation rate distribution and the Holocene mud isopach were developed (Figs. 12, 13). The mud isopach map shows similar spatial patterns to the accumulation rates distribution, their distinguishing feature being a 60-m-thick depocenter in the middle – to – outer shelf (Fig. 13). This depocenter is located along the northern side of the Martaban Depression and on the eastern side of the Sagaing Fault between water depths of 30 m and 130 m (Fig. 13). In the Gulf of Martaban, the mean mud thickness is around 10–20 m. Offshore of the Ayeyarwady River mouths, mud deposits appear significantly thinner, < 15 m in thickness, and are constrained within water depths of 20 m. A mud drape, up to 20 m locally, was found on the northwestern shelf area and, unlike the shelf deposits in the Andaman Sea and Gulf of Martaban, the mud belt in this area gradually extends into the > 300-m deep sea (Fig. 13).

The mud distribution map shows that the Ayeyarwady and Thanlwin river sediments cover > 60,000 km^2 on the shelf, with a calculated total volume of ~1075 km^3 (Table 2). This is equivalent to 1290 × 10^9 tons of sediment in total by using the average sediment dry-bulk density of 1.2 g/cm^3 (1.2 $tons/m^3$). More specifically, there are 120 × 10^9 tons of sediment deposited immediately offshore of the Ayeyarwady River distributaries, 1080 × 10^9 tons in the Gulf of Martaban, and 90 × 10^9 tons in the Northwestern Myanmar Shelf.

4.3. Organic geochemical parameters

The organic geochemistry of sediment samples can reveal information concerning the history of the particles. In general, riverine sediment carries OC derived from terrestrial vascular plants, which will have high lignin contents, relatively high C/N ratios (> 20), and relatively negative $\delta^{13}C$ values (~ −35 to −25‰), and soils that contained more degraded terrestrial OC that is best recognized by lower C/N ratios (~10–13) and oxidized lignin (Goñi et al., 1998). Once introduced to the marine environment, the riverine OC tends to be replaced by marine sources as sediments are transported and stored in surface environments on the seabed (Blair and Aller, 2012). This is recognized by the loss of lignin, a decrease in C/N ratio and a trend to more positive marine $\delta^{13}C$ signatures (~ −18 to −22‰).

Of the eight surface sediment samples we analyzed, one (KC-14) is located immediately offshore of the Ayeyarwady River mouth; two samples (KC-18 and KC-21) are located in the Western Myanmar Shelf, Bay of Bengal; three samples (KC-27, KC-29, and KC-30) are from the Gulf of Martaban; and two samples (KC-23 and KC-24) are from the middle – to – outer shelf offshore of the Ayeyarwady River Delta (Fig. 4 and Table 1). As expected, KC-14, near river mouth, shows the highest C/N ratio (8.5) and lignin phenols content; and the most negative $\delta^{13}C$ (−25‰) (Fig. 14). In contrast, samples KC-23 and KC-24, although they are located in 50–60 m water depth and < 100 km from the Ayeyarwady River mouth, exhibit the lowest C/N ratios (~6.8), the lowest lignin phenol content, and the most positive $\delta^{13}C$ value (−22‰). The samples from Bay of Bengal and Gulf of Martaban display intermediate values. The Gulf of Martaban samples had lower C/N ratio and lower lignin phenols contents than samples from the Bay of Bengal (Fig. 14). Vanillyl phenol acid/aldehyde ratios were highest in samples

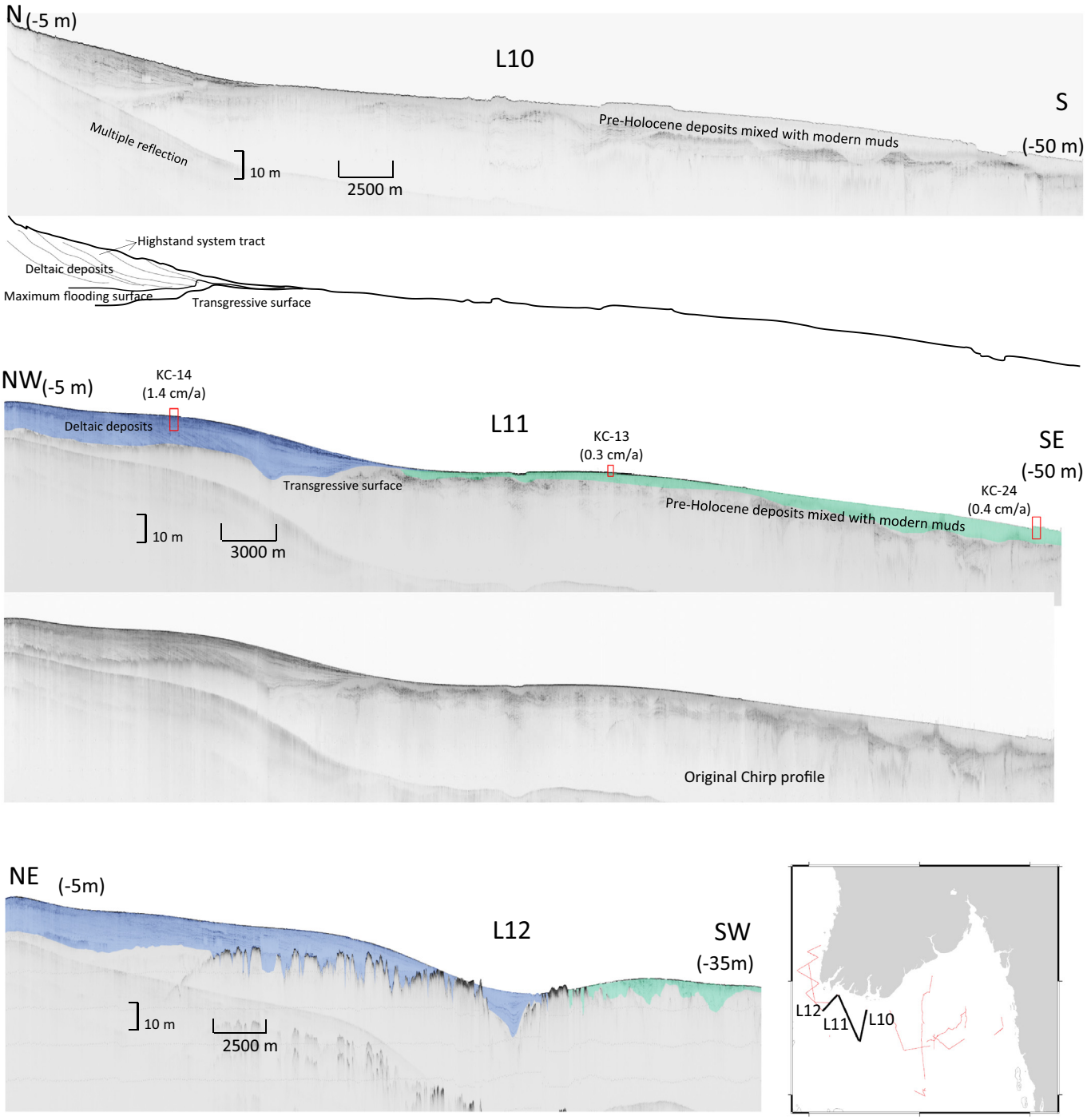

Fig. 8. Chirp-sonar profiles (L10, L11 and L12) immediately offshore of the Ayeyarwady River mouth. These show a very limited cross-shelf (< 25 km in distance, and < 40 m in water depth) distribution of the Holocene mud, only up to 10 m in thickness with a relatively gently sloped foreset.

having the least lignin, reflecting the lignin's highly degraded state (Fig. 14).

5. Discussion

The Ayeyarwady and Thanlwin river sedimentary system is shaped by major tectonic subduction offshore and an extensive and active backarc transform fault passing through its delta plain and adjacent shelf. In this section, we discuss its offshore sediment distribution, accumulation, organic geochemistry, mass budget, and possible sediment transport mechanisms within that context.

5.1. Sediment distribution, transport and accumulation

The selected Chirp-sonar profiles (Figs. 5–11) and 3-D fence diagram (Fig. 9) reveal an extensive modern mud accumulation near the Ayeyarwady and Thanlwin river mouths, in the Gulf of Martaban and Bay of Bengal (Fig. 13). The sediment distribution map shows only a limited amount (~20 of 215 Mt./yr) of the Ayeyarwady River derived sediment that has been accumulated annually near its river mouth (Table 2). Only a small portion of sediment (~15 Mt./yr) was found on the Western Myanmar Shelf. In contrast, a major portion (~180 Mt./yr) has been transported eastward into the Gulf of Martaban. The

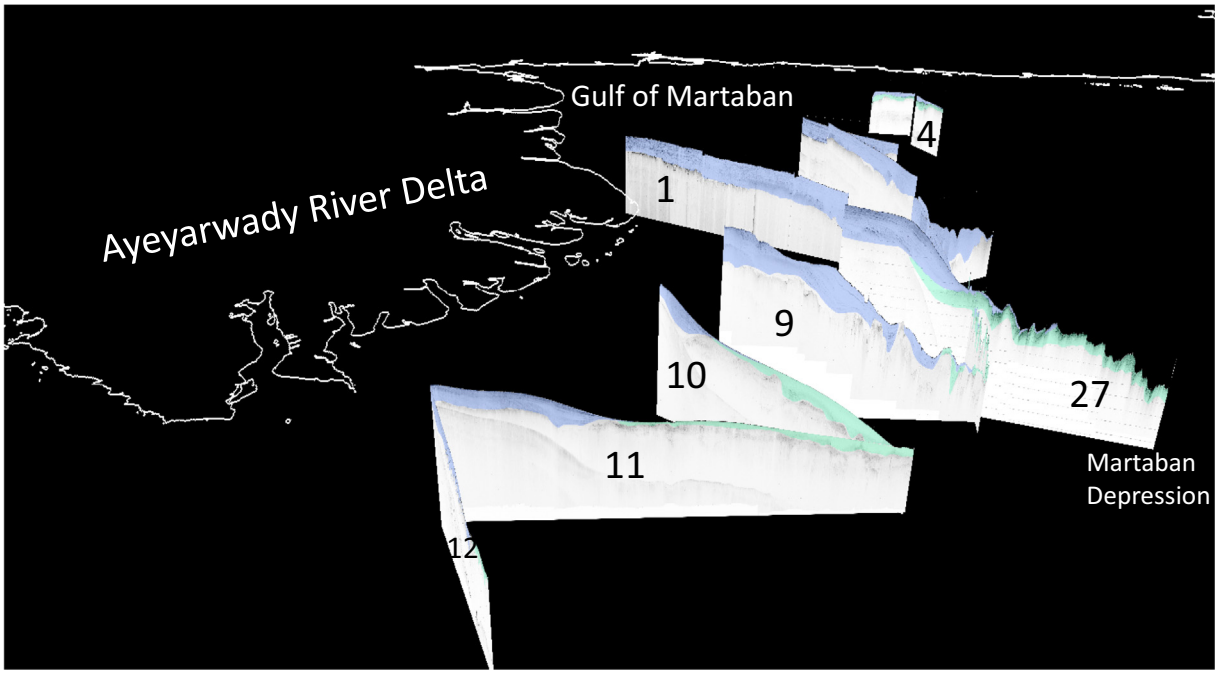

Fig. 9. Fence diagram 3-D view of the Chirp-sonar profiles offshore of the Ayeyarwady River mouth and in the Gulf of Martaban.

schematic sediment accumulation rate distribution map shows accumulation rates in the central Gulf of Martaban to be 0.4–3.0 cm/yr. with the highest depositional rate (3.0 and 10.0 cm/yr) located in the southwestern Gulf of Martaban (Fig. 12). Interestingly, the ^{210}Pb-derived sedimentation rates immediately offshore of the Ayeyarwady and Thanlwin river mouths are only < 1.5 cm/yr. Farther offshore from the Ayeyarwady River mouth, the rates are normally < 0.5 cm/yr. The accumulation rates in the Western Myanmar Shelf off the Rakhine coast

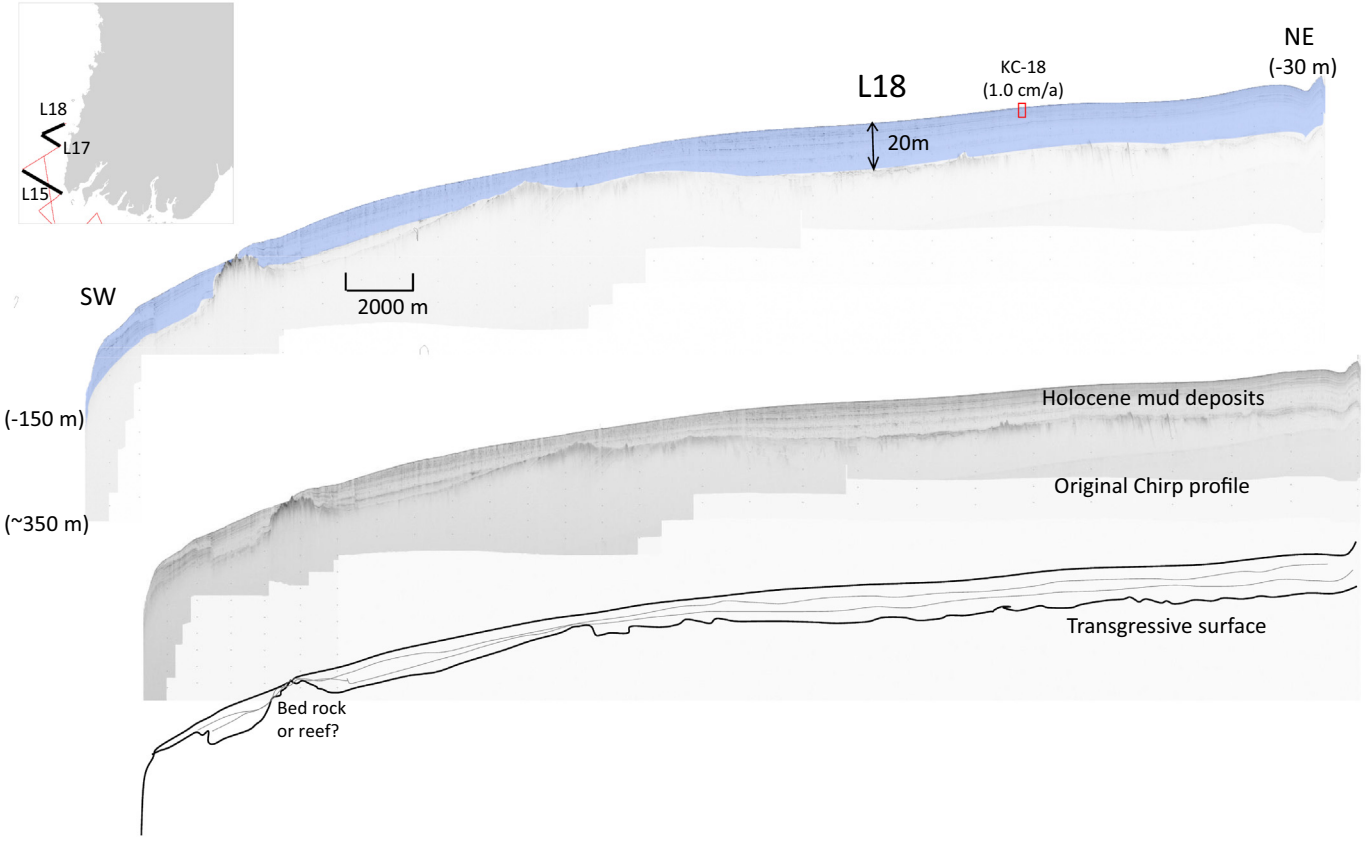

Fig. 10. Cross-shelf Chirp sonar profiles in the Bay of Bengal, west of the Ayeyarwady river delta. Unlike the clinoform in the Gulf of Martaban, here the deposit exhibits a stratified “mud drape or blanket,”

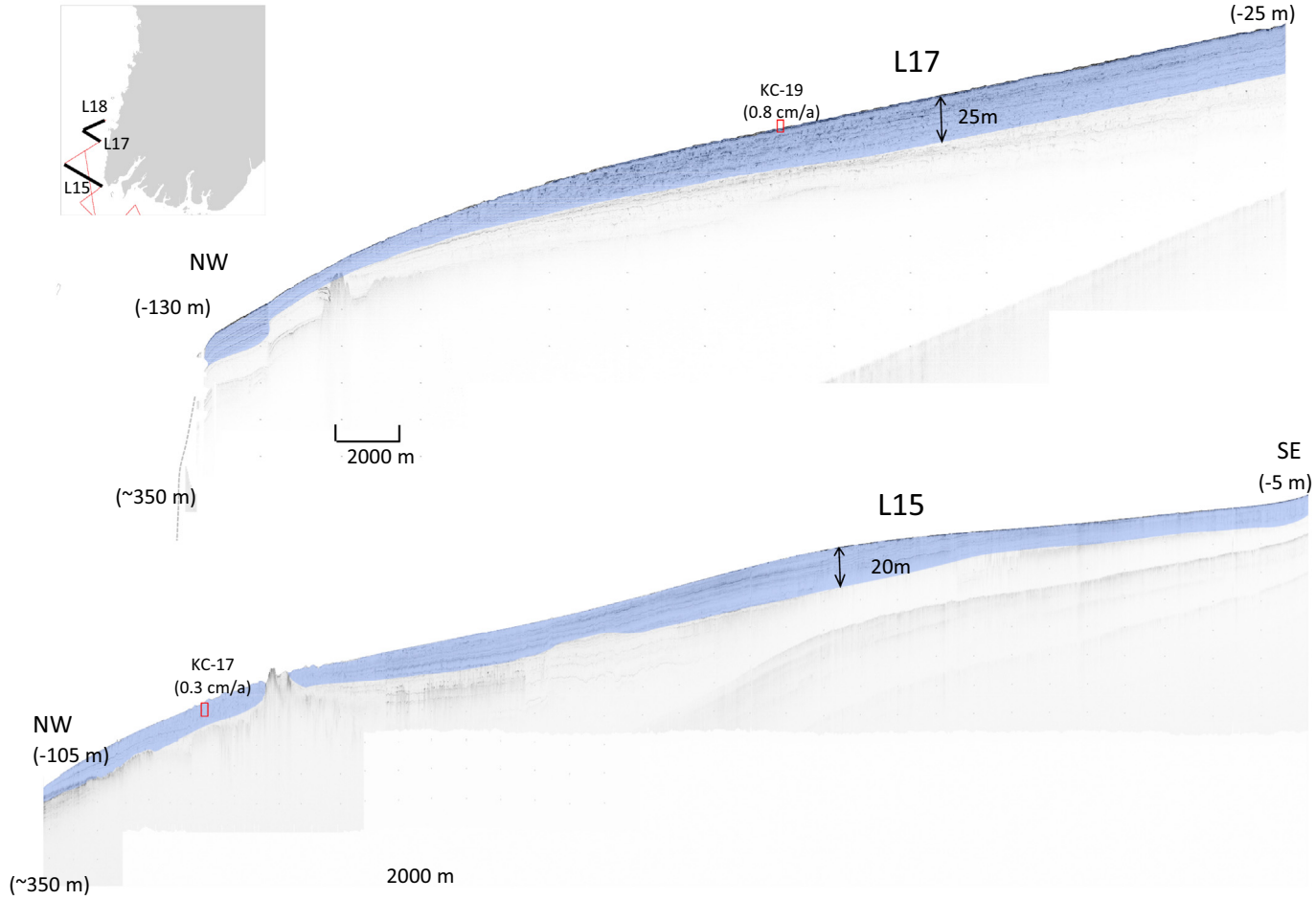

Fig. 10. (*continued*)

are between 0.8 and 1.0 cm/yr (Kuehl et al., 2019). These 100-yr scale accumulation rates are similar to accumulation rates observed offshore of many other major river systems, like the Amazon (Kuehl et al., 1986), Mekong (DeMaster et al., 2017; Liu et al., 2017), Yangtze (Liu et al., 2006), etc.

Most of the mud deposited on the seafloor of the Gulf of Martaban is located between the latitudes of 14.5°N–16°N (Fig. 13), which matches the area observed through satellite images to be covered by turbid water having high suspended sediment concentration (Ramaswamy et al., 2004). Previous studies suggest the extent of the turbid water zone was strongly related to spring-neap tidal cycles. During the spring tide, the turbid zone extended southward to 14.55°N and covered an area > 45,000 km^2; conversely, during the neap tides, the turbid water zone retreated to 16.15°N and only covered 15,000 km^2 (Ramaswamy et al., 2004). A study of 12-years of remote sensing reflectance data shows that the spatial distribution of the highest turbid water zone also responds to the seasonal monsoon. High homogenous SSC covers the entire Gulf of Martaban during the northeast monsoon season while only low and spare SSC was observed during the southwest monsoon seas (Matamin Abd et al., 2015). This indicates that direct river inputs alone do not explain the high turbidity. The local strong oceanographic regime must play some critical roles in maintaining this extensive turbid water zone.

The organic geochemical signatures of sediment collected near the Ayeyarwady River mouth are consistent with those from other world major rivers (Blair and Aller, 2012). The least modified OC, after the river mouth, is found on the Western Myanmar Shelf. This can be explained by the proximity of this location to the river outlet. The Gulf of Martaban organic matter displays a greater replacement of terrestrial OC by marine material, reflecting a longer history in seafloor surface environments that promotes the loss of the terrestrial signal relative to marine inputs, due to the strong resuspension. The inverse relationship between lignin abundance and vanillyl acid/aldehyde ratio indicates that the loss is oxidative and likely the result of long-term residence in surface sediments.

The lignin – $\delta^{13}C$ relationship (Fig. 14) indicates that those two parameters do not track each other perfectly. One explanation is that the lignin parameter is more sensitive to loss than the bulk terrestrial isotopic signal. We speculate that the two parameters follow slightly different trajectories as a result of their respective transport-depositional environments. For instance, sedimentation on the Western Myanmar Shelf may be primarily controlled by a longshore plume and steady sediment settling which would promote preservation of the riverine OC. In addition, episodic input from smaller, local mountainous river could also promote the OC preservation (Damodararao et al., 2016). In contrast, the strong seasonal and tidally-controlled resuspension and along-shelf and cross-shelf redistribution in the Gulf of Martaban would repeatedly expose OC to oxidizing conditions. Supporting those hypotheses, the sediments in the Western Myanmar Shelf are dominated by mottled sand and mud. Sediment in the Gulf of Martaban was found to be extensively mixed to depths of ~1 m below the sediment water interface forming fluid muds, and exhibited a distinctive reddish color that suggest frequent seabed reoxidation (Kuehl et al., 2019).

5.2. No apparent dispersal or accumulation inside the canyon

Previous studies of the suspended sediment concentration have

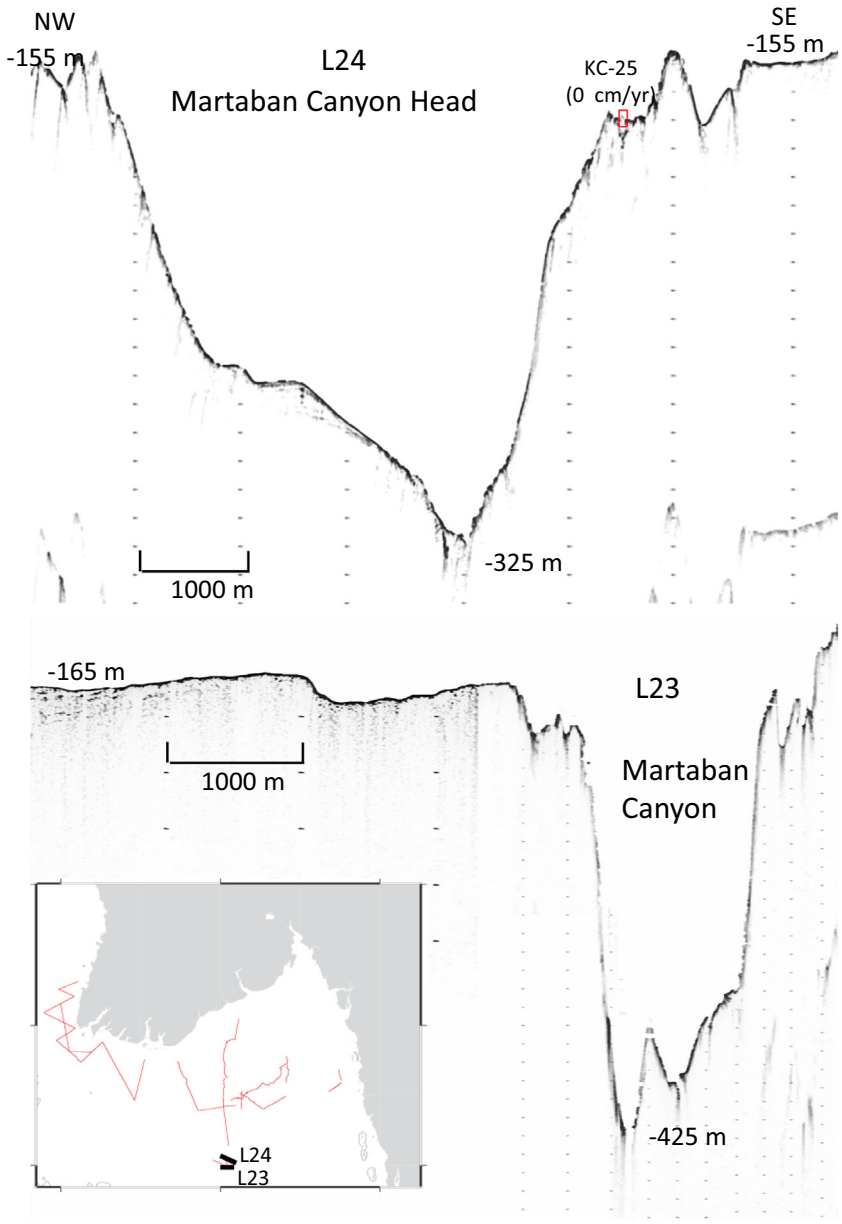

Fig. 11. Selected Chirp sonar profiles crossing the Martaban Canyon indicate there is no modern mud accumulation.

indicated that there might be a nepheloid layer near the bottom with SSC up to 1 mg/l between water depths of 100–150 m (Ramaswamy et al., 2004). Surface sediments from the Martaban Canyon indicate the canyon floor is mainly covered by sand mixed with silty sand and silty clay (Rao et al., 2005). Therefore Ramaswamy and Rao (2014) proposed that a portion of the Ayeyarwady-Thanlwin riverine sediments might be transported into the Martaban Canyon and farther to the deep Andaman Sea. However, our Chirp-sonar profiles that crossed the 400–500-m-deep canyon did not show any apparent modern mud accumulation, progradation, draping or slumping; neither in the bottom of the canyon at water depths of 300–500 m, nor its shallow banks at 150–170-m water depths (Fig. 11). Of course, since we were unable to collect Chirp-sonar profiles of the seafloor at in the deep Andaman Sea, we cannot say that there is absolutely no modern mud accumulation there. Furthermore, we also did not observe any distinct mud accumulation seaward of the modern mud wedge in water depths between 130 and 500 m, based on our Chirp-sonar profiles. Additionally, a sediment core, SK-234-60, collected from the central Andaman Sea at a water depth of 2000 m shows the thickness of the Holocene mud accumulation over the past 8 kyr to be only 0.55 m (Awasthi et al., 2014), which indicates a significantly lower accumulation rate of 0.007 cm/yr compared to the rates on the shelf of 1.0–10 cm/yr (Fig. 12). A similar rate was found from the core RC12-344 in the Andaman Sea, which had a 0.58-cm mud deposit formed over 7 kyr (Rashid et al., 2007). Therefore, if there is any sediment escaping to the deep Andaman Sea, the flux seems insignificant, compared to the accumulation on the shelf.

5.3. Possible sediment transport and depositional mechanisms

From the geophysical and geochemical data (Figs. 12, 13, 14) we see that the Ayeyarwady River derived sediments do not transport across shelf, and no apparent modern accumulation was detected on the Chirp-sonar profiles (Figs. 8-9), and the sediment accumulation rate and terrestrial OC contents were also very low (Figs. 12, 13, 14). The majority of the riverine sediment was deposited in the Gulf of Martaban (Table 2), and a mud drape was also found to accumulate on the Western Myanmar Shelf of the eastern Bay of Bengal. Study of the beach

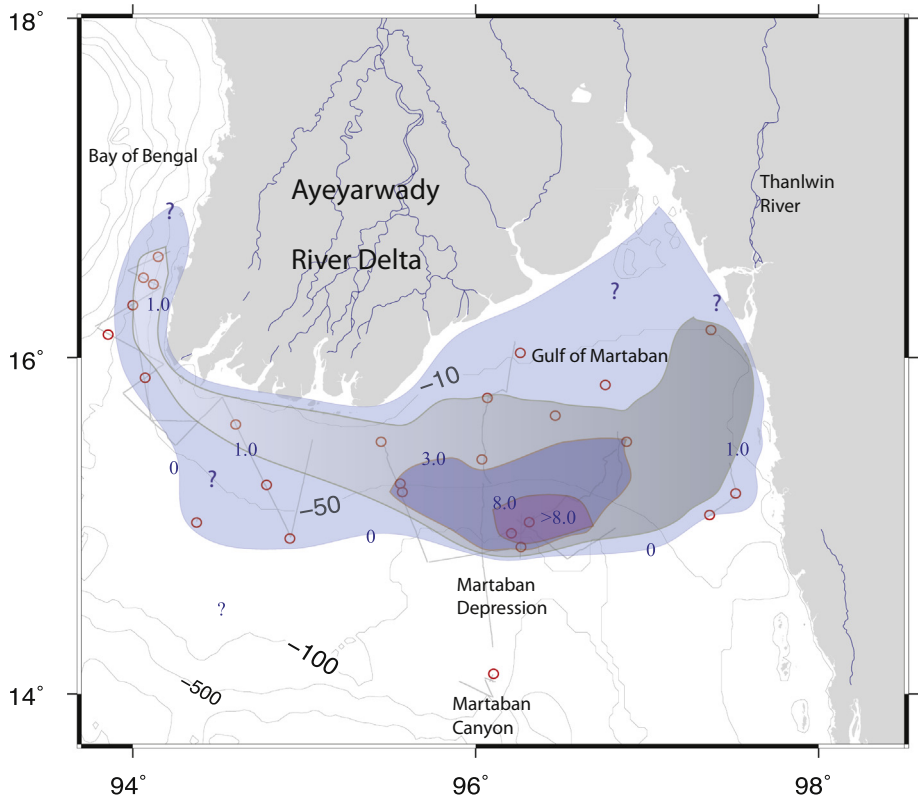

Fig. 12. ^{210}Pb derived Sediment Accumulation Rates (SAR) distribution on the shelf offshore of the Ayeyarwady River Delta. (Data from Kuehl et al., 2019.)

and neashore profiles indicates that sediments delivered from the Ayeyarwady distributary mouths are mainly transported eastward to the Gulf of Martaban by waves and currents (Anthony et al., 2017, 2019), the reversed currents flowing westward were observed locally (Besset et al., 2017).

Therefore, we speculate that during the SW monsoon, wind – driven currents transport the Ayeyarwady River plume eastward into the Gulf of Martaban. During this time, waves are especially energetic on near the distributary mouths (Kuehl et al., 2019); so waves and tidal currents rework and re-suspend the sediments previously deposited near the river's distributary mouths. This would winnow the nearshore environments of the Ayeryarwady River mouth, and deliver fine sediment

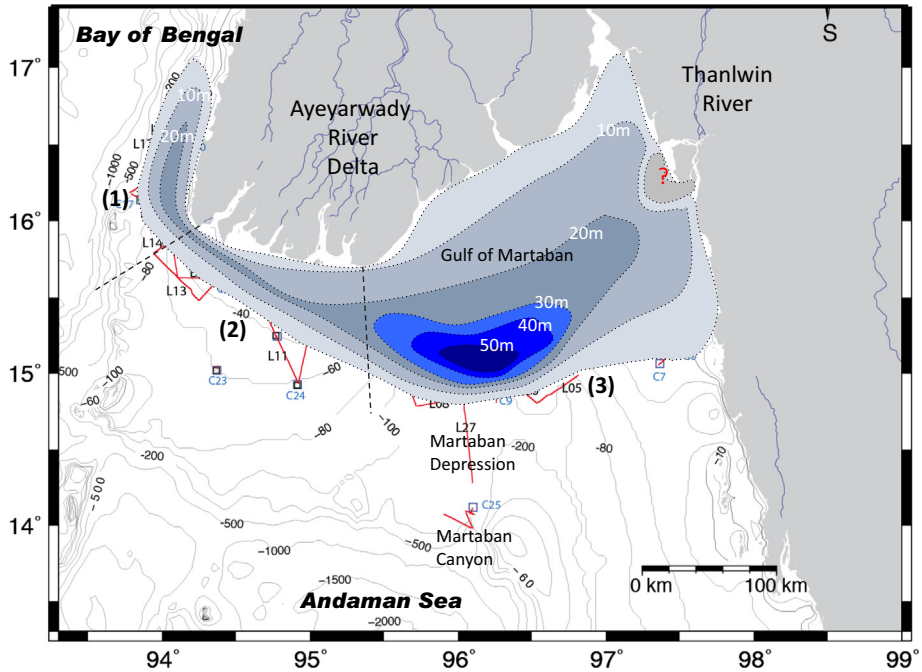

Fig. 13. Isopach map of the late-Holocene Ayeyarwady and Thanlwin derived mud accumulation on the Gulf of Martaban and Bay of Bengal. Two dashed lines seperate the study area into three areas as discussed in Table 2.

Table 2
Summary of the modern Ayeyarwady and Thanlwin subaqueous delta characteristics, based on the analyses of Chirp-sonar profiles and isopach map shown in Fig. 13.

	(1) Western Myanmar shelf	(2) Shelf off the Ayeyarwady River mouths	(3) Gulf of Martaban	Total
Mud cover area (km^2)	5000	10,000	45,000	60,000
Maximum water depth (m)	> 300	30	130	
Maximum thickness (m)	20	15	60	
^{210}Pb-derived accumulation rates (cm/yr)	0.3–1.0	0.4–1.4	0.3–9.4	
Estimated volume ($\times 10^9$ m^3)	75	100	900	1075
Estimated mass ($\times 10^9$ ton)	90	120	1080	1290
Annual flux (Mt/yr)	15 (7%)	20 (10%)	180 (83%)	215

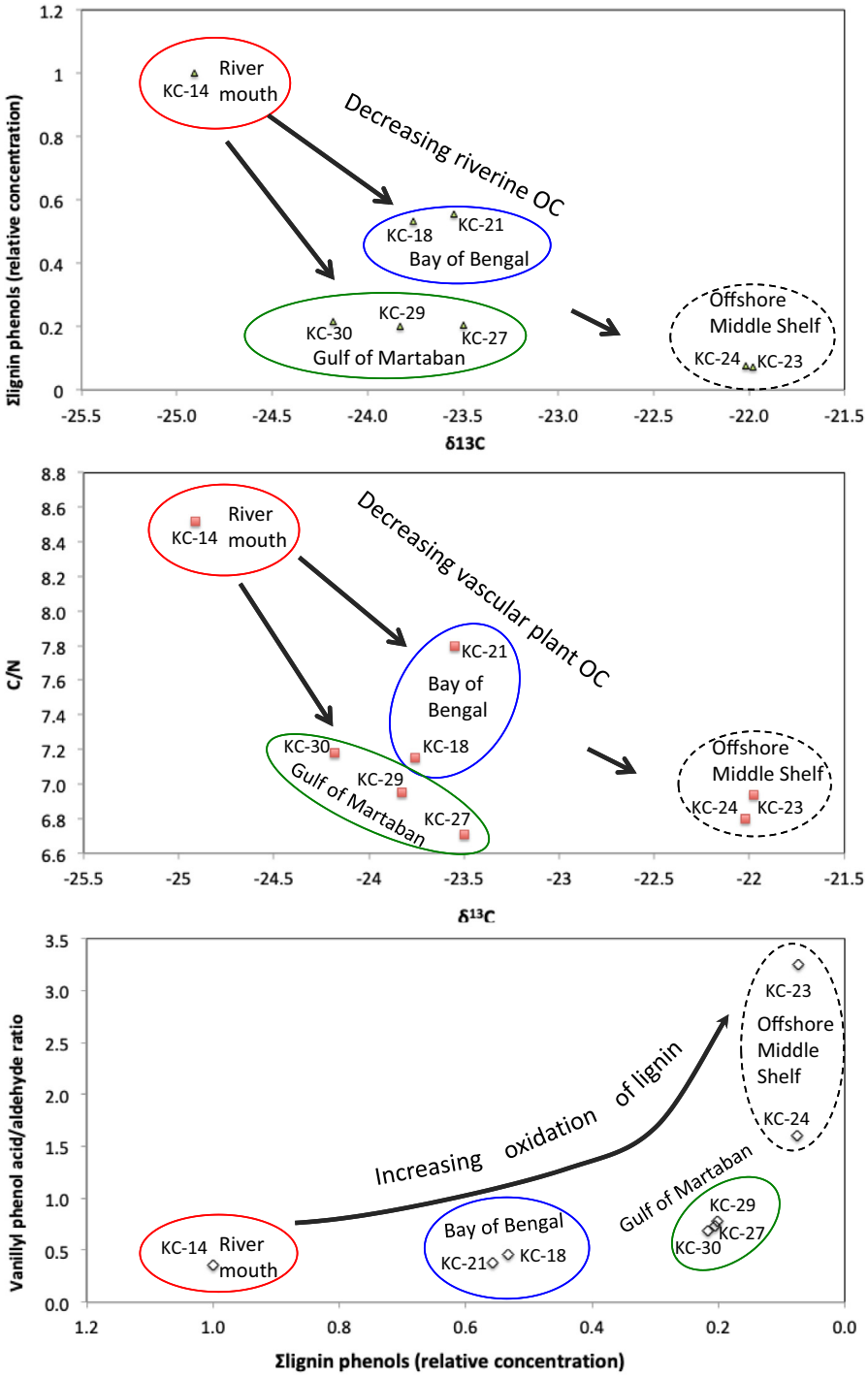

Fig. 14. The relationships between $\delta^{13}C$, C/N, the sum of lignin phenols (normalized), and lignin vanillyl acid/aldehyde ratios based on the organic carbon geochemical analyses of the samples from the river mouth, middle shelf, Gulf of Martaban, and Bay of Bengal. Sample locations are shown in Fig. 4.

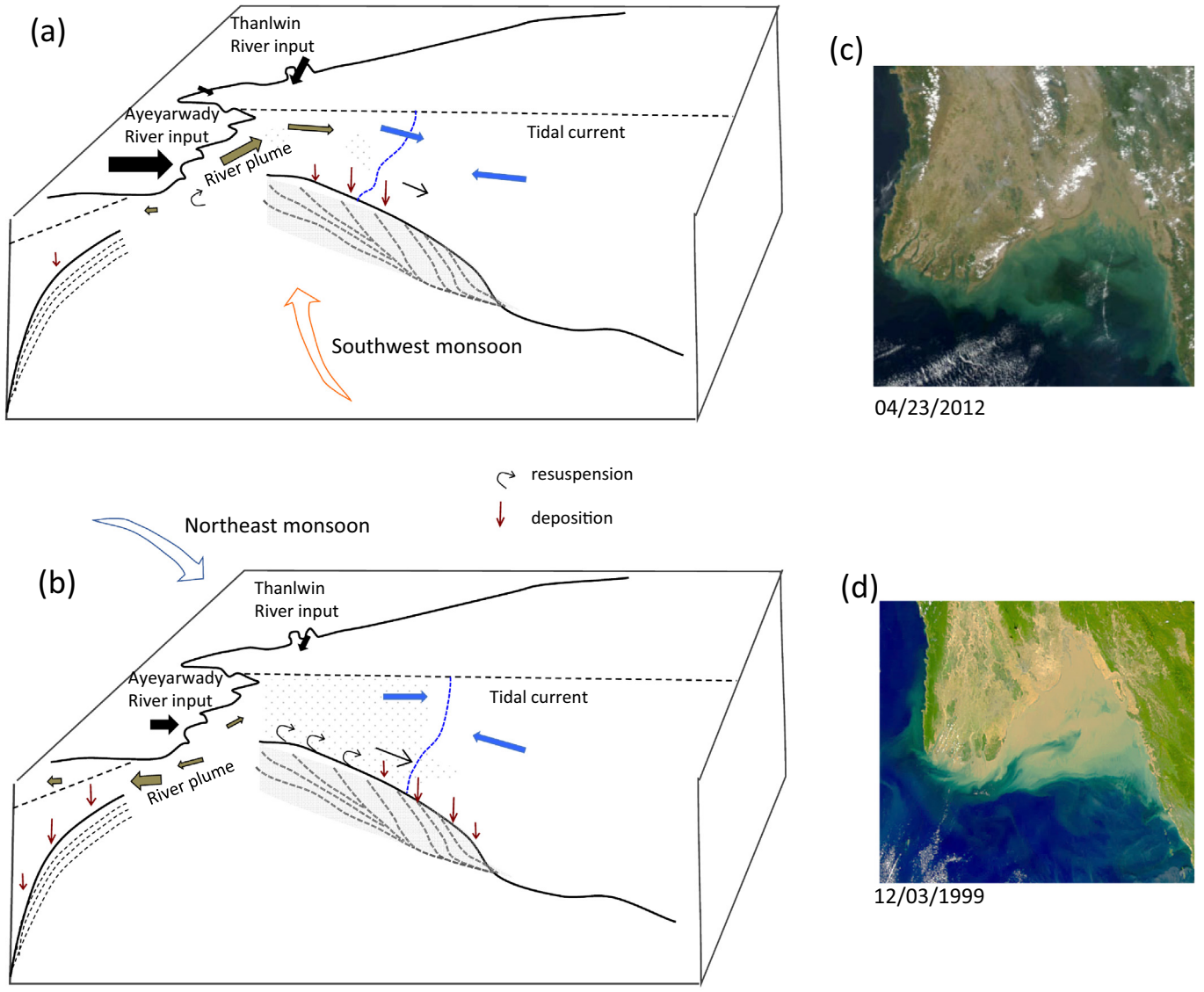

Fig. 15. Conceptual cartoon showing hypothesized sediment source, transport and deposit from the Ayeyarwady and Thanlwin rivers to the Gulf of Martaban and Bay of Bengal under the SW monsoon (a) and NE monsoon (b), (c) Satellite image acquire in April 2012 (d) Satellite image acquire in December 1999 (source http://www.eosnap.com).

to the Gulf of Martaban. During the NE monsoon season, wave energy is weaker (Kuehl et al., 2019), but strong tidal currents would resuspend fine sediments previously accumulated in the shallow portion of the Gulf of Martaban. Offshore directed winds during the NE monsoon would increase the footprint of the surface turbid water zone, compared to the shoreward directed winds of the SW monsoon season, which might trap the surface turbid water closer to shore. This may explain why the footprint of the surface turbid water reaches the maximum during the NE monsoon season. Satellite images show that during the NE monsoon, surface currents carry turbid water into the Bay of Bengal which encourages deposition along the Western Myanmar Shelf (Fig. 15). Geochemical data of Sr and Nd isotope compositions show local rivers like Kaladan, Naf, and other small rivers might also deliver sediment to the nearby Western Myanmar Shelf, but the impacts of G-B river system on the Myanmar shelf seems to be quite minimal (Damodararao et al., 2016). Our organic carbon geochemical data support the gradual change or degradation from the river mouth the Gulf of Martaban and to the Bay of Bengal (Fig. 14).

Another possible mechanism for delivering significant amounts of sediment from the river mouths to the sea is tropical cyclones. For instance, during Tropical Cyclone Nargis in May 2008, the offshore suspended particular matter (SPM) increased sharply compared to the past 10-year monthly mean. During the passage of Nargis, over the delta region, the average SSC increased nearly 50%, and the highly turbid water was maintained in the Gulf of Martaban for nearly two months (Besset et al., 2017), which might have been the results of large river discharge with high SSC and the strong local resuspension in the gulf. A similar mechanism was also observed in the East China Sea, during typhoon Morakot in August 2009. Turbidity in the water column along the Yangtze River derived mud belt increased to more than ten-fold greater than pre-typhoon values (Li et al., 2012). Typhoon Saola in August 2012 strongly disturbed and re-worked the mud deposit in the inner shelf of the East China Sea and generated a 10–25 cm thick storm-deposited layer (Li et al., 2015). Similarly, during the tropical Cyclone Sidr in November 2007, massive amount of sediment was delivered from the shelf of Ganges-Brahmaputra to the Bay of Bengal (Roger and Goodbred, 2010). Therefore we speculate that tropical storms play a major role in delivering the sediment to the sea and helping form the distinct clinoform in the Martaban Depression.

5.4. Comparison with other Asian large-river delta systems

Sediments from most of the East Asian river systems are delivered during the summer monsoon season; however, they are only deposited near their river mouths temporarily. The majority of the sediment is resuspended and transported along the shore, contributing to the elongated mud belt with a distal mud depocenter, much like the Yellow, Yangtze, Pearl and Mekong Rivers (see Liu et al., 2009, 2017). Upon reaching the coast, these rivers' sedimentary systems show winter-monsoon-dominated, unidirectional longshore transport that extends 300–800-km from the river mouths. In contrast, the Ayeyarwady River sedimentary system shows a bi-directional transport under the SW and NE monsoons, respectively (Kuehl et al., 2019). The adjacent G-B river delta system shares many distinguishing features with the Ayeyarwady River system, such as high sediment discharge, a confined bay area, and a tectonically controlled canyon system. High-resolution Chirp-sonar profiles indicate that a large portion of the G-B river derived sediment is actively transported into its adjacent canyon system and dispersed further in the deep Bay of Bengal (Kuehl et al., 1997; Rogers and Goodbred, 2010; Rogers et al., 2015). Using the same technology of Chirp-sonar surveys, in this study we did not find any significant mud being transported, slumped, or deposited in Martaban Canyon (Figs. 11, 13). This lack of sedimentation in the canyon could be explained by sediment retention in the gulf by local strong tidal currents and estuarine-like seasonal circulation (Fig. 15). Though we have not identified any major sediment flux to Martaban Canyon, in the Western Myanmar Shelf, sediment may escape off the slope and even reach the adjacent Andaman Sea subduction trench in the eastern Bay of Bengal (Figs. 10, 15).

6. Conclusions

1) An extensively distributed mud deposit, covering up to 60,000 km^2 was found that extended into the Gulf of Martaban, and the shelves offshore of the Ayeyarwady River mouths and Western Myanmar Shelf in the Bay of Bengal.
2) The Chirp-sonar profiles indicated that sediment accumulation immediately offshore of the Ayeyarwady River mouths accounts for only a modest portion of the sediment budget. Rather, the majority of sediment was deposited in the Gulf of Martaban as a distal mud depocenter, with local thicknesses up to 60 m. In the Western Myanmar Shelf, offshore of the Rakhine coast, we found a mud drape extending from the nearshore to the 300-m deep slope. The sediment accumulation rates in the distal depocenter were as high as 3.0–10 cm/yr, while the rates in other mud-dominated areas ranged from 0.3 to 1.5 cm/yr. Organic geochemical signatures for riverine OC decrease as sediment is transported from the source. Relationships between the various parameters suggested that sediment is transiting through one of two different depositional environments, one characterized by steady accumulation and the other by frequent resuspension-deposition cycles as exhibited by fluid muds.
3) The fates of Ayeyarwady and Thanlwin river derived sediments appear to fit a bi-directional transport model. During the SW monsoon season, the river discharges 80% its sediment load, but the tide and coastal currents transport the buoyant river plume eastward and encourage sediment accumulation in the Gulf of Martaban. In the NE monsoon season, the previously deposited fine mud becomes resuspended and transported further offshore into the Martaban Depression. The coastal current may transport some suspended mud westward into the Bay of Bengal, providing a source for deposition along the Western Myanmar Shelf.
4) The total mud accumulated in the survey is about 1290×10^9 tons, which suggests a historical annual mean depositional rate of 215 Mt./yr. This accounts for about 1/3 of the modern Ayeyarwady and Thanlwin rivers derived sediment, the remaining 2/3 has been accumulated and built the subaerial delta plain in the past 6000 years.
5) The Chirp-sonar profiles crossing the Martaban Canyon between 300 and 500 m water depths did not reveal any modern mud accumulation at the canyon floors or banks. The profiles between the canyon head and Martaban Depression also did not show any modern sedimentation; rather, only relict sand-dominated deposits.
6) More in-situ, sediment dynamic observations and modeling simulation works are needed to gather a more complete understanding of the seasonal and annual sediment transport from the river to the sea.

Acknowledgement

This project was funded by the US National Science Foundation under grants OCE-1737287 (Liu) and OCE-1737221 (Kuehl and Harris), and Office of Naval Research grant (N000141712907). We thank colleagues from the Yangon University and Mawlamyine University for the joint cruise, and appreciate the help from the RV Sea Princes crewmembers. Mary Goodwyn and Danielle Tarpley at VIMS helped the cruise and sampling, Jieun Kim at Northwestern University provided the lignin measurements, and the manuscript benefitted from discussion with Matthew Fair (VIMS Contribution No. 3872). We are especially giving thanks to three anonymous reviewers for their insightful comments and constructive suggestions.

References

Alexander, C.R., DeMaster, D.J., Nittrouer, C.A., 1991. Sediment accumulation in a modern epicontinental-shelf setting: the Yellow Sea. Mar. Geol. 98, 51–72. https://doi.org/10.1016/0025-3227(91)90035-3.

Anthony, E.J., Besset, M., Dussouillez, P., 2017. Recent Shoreline Changes and Morpho-Sedimentary Dynamics of the Ayeyarwady River Delta: Assessing the Impact of Anthropogenic Activities on Delta Shoreline Stability. WWF Asia and Helmsley Foundation, Yangon, Myanmar, pp. 43.

Anthony, E.J., Besset, M., Dussouillez, P., Goichot, M., Loisel, H., 2019. Overview of the Monsoon-influenced Ayeyarwady River delta, and delta shoreline mobility in response to changing fluvial sediment supply. Mar. Geol. 106038. https://doi.org/10.1016/j.margeo.2019.106038.

Awasthi, N., Ray, J.S., Singh, A.K., Band, S.T., Rai, V.K., 2014. Provenance of the Late Quaternary sediments in the Andaman Sea: Implications for monsoon variability and ocean circulation. Geochem. Geophys. Geosyst. 15, 3890–3906. https://doi.org/10.1002/2014gc005462.

Besset, M., Anthony, E.J., Dussouillez, P., Goichot, M., 2017. The impact of Cyclone Nargis on the Ayeyarwady (Irrawaddy) river delta shoreline and nearshore zone (Myanmar): towards degraded delta resilience? Compt. Rendus Geosci. 349, 238–247. https://doi.org/10.1016/j.crte.2017.09.002.

Bird, M.I., Robinson, R.A.J., Win Oo, N., Maung Aye, M., Lu, X.X., Higgitt, D.L., Swe, A., Tun, T., Lhaing Win, S., Sandar Aye, K., Mi Mi Win, K., Hoey, T.B., 2008. A preliminary estimate of organic carbon transport by the Ayeyarwady (Irrawaddy) and Thanlwin (Salween) Rivers of Myanmar. Quat. Int. 186, 113–122. https://doi.org/10.1016/j.quaint.2007.08.003.

Blair, N.E., Aller, R.C., 2012. The fate of Terrestrial Organic Carbon in the marine environment. Annu. Rev. Mar. Sci. 4, 401–423. https://doi.org/10.1146/annurev-marine-120709-142717.

Chapman, H., Bickle, M., Thaw, S.H., Thiam, H.N., 2015. Chemical fluxes from time series sampling of the Irrawaddy and Salween Rivers, Myanmar. Chem. Geol. 401, 15–27. https://doi.org/10.1016/j.chemgeo.2015.02.012.

Clift, P.D., Giosan, L., Henstock, T.J., Tabrez, A.R., 2014. Sediment storage and reworking on the shelf and in the Canyon of the Indus River-Fan System since the last glacial maximum. Basin Res. 26, 183–202. https://doi.org/10.1111/bre.12041.

Coplen, T.B., 2011. Guidelines and recommended terms for expression of stable-isotope-ratio and gas-ratio measurement results. Rapid Commun Mass Sp 25 (17), 2538–2560. https://doi.org/10.1002/rcm.5129.

Craig, H., 1953. The geochemistry of the stable carbon isotopes. Geochim Cosmochim Ac 3 (2–3), 53–92. https://doi.org/10.1016/0016-7037(53)90001-5.

Cui, L., Butler, H.J., Martin-Hirsch, P.L., Martin, F.L., 2016. Aluminium foil as a potential substrate for ATR-FTIR, transflection FTIR or Raman spectrochemical analysis of biological specimens. Anal. Methods 8 (3), 481–487. https://doi.org/10.1039/c5ay02638e.

Curray, J.R., 2005. Tectonics and history of the Andaman Sea region. J. Asian Earth Sci. 25, 187–232. https://doi.org/10.1016/j.jseaes.2004.09.001.

Damodararao, K., Singh, S.K., Rai, V.K., Ramaswamy, V., Rao, P.S., 2016. Lithology, monsoon and sea-surface current control on provenance, dispersal and deposition of sediments over the Andaman Continental Shelf. Frontiers in Marine Science 3. https://doi.org/10.3389/fmars.2016.00118.

DeMaster, D.J., Liu, J.P., Eidam, E., Nittrouer, C.A., Nguyen, T.T., 2017. Determining rates of sediment accumulation on the Mekong shelf: timescales, steady-state

assumptions, and radiochemical tracers. Cont. Shelf Res. 147, 182–196. https://doi.org/10.1016/j.csr.2017.06.011.
Fournillier, K., 2016. A Multiple Tracer Approach to Tracking Changes in Terrestrial Organic Carbon Transported Across a Small Mountainous River Landscape Using Deuterated Tetramethylammonium Hydroxide Thermochemolysis. Northwestern University, ProQuest Dissertations Publishing.
Fritz, H.M., Blount, C.D., Thwin, S., Thu, M.K., Chan, N., 2009. Cyclone Nargis storm surge in Myanmar. Nat. Geosci. 2, 448. https://doi.org/10.1038/ngeo558. https://www.nature.com/articles/ngeo558.
Furuichi, T., Win, Z., Wasson, R.J., 2009. Discharge and suspended sediment transport in the Ayeyarwady River, Myanmar: centennial and decadal changes. Hydrol. Process. 23, 1631–1641. https://doi.org/10.1002/Hyp.7295.
Gao, S., Liu, Y., Yang, Y., Liu, P.J., Zhang, Y., Wang, Y.P., 2015. Evolution status of the distal mud deposit associated with the Pearl River, northern south China sea continental shelf. J. Asian Earth Sci. 114 (Part 3), 562–573. https://doi.org/10.1016/j.jseaes.2015.07.024.
Ge, Q., Liu, J.P., Xue, Z., Chu, F., 2014. Dispersal of the Zhujiang River (Pearl River) derived sediment in the Holocene. Acta Ocean. Sin. 33, 1–9. https://doi.org/10.1007/s13131-014-0407-8.
Giosan, L., Constantinescu, S., Clift, P.D., Tabrez, A.R., Danish, M., Inam, A., 2006. Recent morphodynamics of the Indus delta shore and shelf. Cont. Shelf Res. 26, 1668–1684. https://doi.org/10.1016/j.csr.2006.05.009.
Giosan, L., Naing, T., Min Tun, M., Clift, P.D., Filip, F., Constantinescu, S., Khonde, N., Blusztajn, J., Buylaert, J.P., Stevens, T., Thwin, S., 2018. On the Holocene evolution of the Ayeyawady megadelta. Earth Surf. Dynam. 6, 451–466. https://doi.org/10.5194/esurf-6-451-2018.
Goñi, M.A., Ruttenberg, K.C., Eglinton, T.I., 1998. A reassessment of the sources and importance of land-derived organic matter in surface sediments from the Gulf of Mexico. Geochim. Cosmochim. Acta 62 (18), 3055–3075.
Goodbred, S.L., Kuehl, S.A., 2000. The significance of large sediment supply, active tectonism, and eustasy on margin sequence development: Late Quaternary stratigraphy and evolution of the Ganges-Brahmaputra delta. Sediment. Geol. 133, 227–248. https://doi.org/10.1016/S0037-0738(00)00041-5.
Grill, G., Lehner, B., Thieme, M., Geenen, B., Tickner, D., Antonelli, F., Babu, S., Borrelli, P., Cheng, L., Crochetiere, H., Ehalt Macedo, H., Filgueiras, R., Goichot, M., Higgins, J., Hogan, Z., Lip, B., McClain, M.E., Meng, J., Mulligan, M., Nilsson, C., Olden, J.D., Opperman, J.J., Petry, P., Reidy Liermann, C., Sáenz, L., Salinas-Rodríguez, S., Schelle, P., Schmitt, R.J.P., Snider, J., Tan, F., Tockner, K., Valdujo, P.H., van Soesbergen, A., Zarfl, C., 2019. Mapping the world's free-flowing rivers. Nature 569, 215–221. https://doi.org/10.1038/s41586-019-1111-9.
Hanebuth, T.J.J., Lantzsch, H., Nizou, J., 2015. Mud depocenters on continental shelves—appearance, initiation times, and growth dynamics. Geo-Mar. Lett. 35, 487–503.
Hedley, P.J., Bird, M.I., Robinson, R.A.J., 2010. Evolution of the Irrawaddy delta region since 1850. Geogr. J. 176, 138–149. https://doi.org/10.1111/j.1475-4959.2009.00346.x.
Kuehl, S.A., Demaster, D.J., Nittrouer, C.A., 1986. Nature of sediment accumulation on the Amazon continental shelf. Cont. Shelf Res. 6, 209–225. https://doi.org/10.1016/0278-4343(86)90061-0.
Kuehl, S.A., Levy, B.M., Moore, W.S., Allison, M.A., 1997. Subaqueous delta of the Ganges-Brahmaputra river system. Mar. Geol. 144, 81–96. https://doi.org/10.1016/S0025-3227(97)00075-3.
Kuehl, S.A., Williams, J., Liu, J.P., Harris, C., Aung, D.W., Tarpley, D., Goodwyn, M., Aye, Y.Y., 2019. Sediment dispersal and accumulation off the Ayeyarwady delta – Tectonic and oceanographic controls. Mar. Geol. 10600. https://doi.org/10.1016/j.margeo.2019.106000.
Leithold, E.L., Blair, N.E., Childress, L.B., Brulet, B.R., Marden, M., Orpin, A.R., Kuehl, S.A., Alexander, C.R., 2013. Signals of watershed change preserved in organic carbon buried on the continental margin seaward of the Waipaoa River, New Zealand. Mar. Geol. 346, 355–365. https://doi.org/10.1016/j.margeo.2013.10.007.
Li, Y., Wang, A., Qiao, L., Fang, J., Chen, J., 2012. The impact of typhoon Morakot on the modern sedimentary environment of the mud deposition center off the Zhejiang–Fujian coast, China. Cont. Shelf Res. 37, 92–100. https://doi.org/10.1016/j.csr.2012.02.020.
Li, Y., Li, H., Qiao, L., Xu, Y., Yin, X., He, J., 2015. Storm deposition layer on the Fujian coast generated by Typhoon Saola (2012). Sci. Rep.-UK 5, 14904. https://doi.org/10.1038/srep14904.
Liu, J.P., Milliman, J.D., Gao, S., Cheng, P., 2004. Holocene development of the Yellow River subaqueous delta, North Yellow Sea. Mar. Geol. 209, 45–67. https://doi.org/10.1016/j.margeo.2004.06.009.
Liu, J.P., Li, A.C., Xu, K.H., Veiozzi, D.M., Yang, Z.S., Milliman, J.D., DeMaster, D., 2006. Sedimentary features of the Yangtze River-derived along-shelf clinoform deposit in the East China Sea. Cont. Shelf Res. 26, 2141–2156.
Liu, J.P., Xu, K., Li, A., Milliman, J., Velozzi, D., Xiao, S., Yang, Z., 2007. Flux and fate of Yangtze river sediment delivered to the East China Sea. Geomorphology 85, 208–224. https://doi.org/10.1016/j.geomorph.2006.03.023.
Liu, J.P., Xue, Z., Ross, K., Wang, H., Yang, Z., Li, A., Gao, S., 2009. Fate of sediments delivered to the sea by Asian large rivers: long-distance transport and formation of remote alongshore clinothems. The Sedimentary Record 7, 4–9.
Liu, J.P., DeMaster, D.J., Nittrouer, C.A., Eidam, E.F., Nguyen, T.T., 2017. A seismic study of the Mekong subaqueous delta: proximal versus distal sediment accumulation. Cont. Shelf Res. 147, 197–212. https://doi.org/10.1016/j.csr.2017.07.009.
Matamin Abd, R., Ahmad, F., Mamat, M., Abdullah, K., Harun, S., 2015. Remote Sensing of Suspended Sediment Over Gulf of Martaban, Ekologia. pp. 54.
Milliman, J.D., Farnsworth, K.L., 2011. River Discharge to the Coastal Ocean: A Global Synthesis. Cambridge University Press, Cambridge; New York.
Morley, C.K., 2013. Discussion of tectonic models for Cenozoic strike-slip fault-affected continental margins of mainland SE Asia. J. of Asian Earth Sci. 76, 137–151. https://doi.org/10.1016/j.jseaes.2012.10.019.
Ota, Y., Kawahata, H., Murayama, M., Inoue, M., Yokoyama, Y., Miyairi, Y., Aung, T., Hassain, H.M.Z., Suzuki, A., Kitamura, A., Moe, K., 2017. Effects of intensification of the Indian Summer Monsoon on northern Andaman Sea sediments during the past 700 years. J. Quat. Sci. 32, 528–539. https://doi.org/10.1002/jqs.2947.
Patruno, S., Hampson, G.J., Jackson, C.A.L., 2015. Quantitative characterisation of deltaic and subaqueous clinoforms. Earth Sci. Rev. 142, 79–119. https://doi.org/10.1016/j.earscirev.2015.01.004.
Ramaswamy, V., Rao, P.S., 2014. Chapter 17 the Myanmar continental shelf. Geological Society, London, Memoirs 41, 231–240.
Ramaswamy, V., Rao, P.S., Rao, K.H., Thwin, S., Rao, N.S., Raiker, V., 2004. Tidal influence on suspended sediment distribution and dispersal in the northern Andaman Sea and Gulf of Martaban. Mar. Geol. 208, 33–42. https://doi.org/10.1016/j.margeo.2004.04.019.
Ramaswamy, V., Gaye, B., Shirodkar, P.V., Rao, P.S., Chivas, A.R., Wheeler, D., Thwin, S., 2008. Distribution and sources of organic carbon, nitrogen and their isotopic signatures in sediments from the Ayeyarwady (Irrawaddy) continental shelf, northern Andaman Sea. Mar. Chem. 111, 137–150. https://doi.org/10.1016/j.marchem.2008.04.006.
Rao, P.S., Ramaswamy, V., Thwin, S., 2005. Sediment texture, distribution and transport on the Ayeyarwady continental shelf, Andaman Sea. Mar. Geol. 216, 239–247. https://doi.org/10.1016/J.Margeo.2005.02.016.
Rashid, H., Flower, B.P., Poore, R., Quinn, T.M., 2007. A ~25 ka Indian Ocean monsoon variability record from the Andaman Sea. Quaternary Science Reviews - Quaternary Sci Rev 26, 2586–2597. https://doi.org/10.1016/j.quascirev.2007.07.002.
Robinson, R.A.J., Bird, M.I., Oo, N.W., Hoey, T.B., Aye, M.M., Higgitt, D.L., Lu, X.X., Swe, A., Tun, T., Win, S.L., 2007. The Irrawaddy River sediment flux to the Indian Ocean: the original nineteenth-century data revisited. J. Geol. 115, 629–640. https://doi.org/10.1086/521607.
Rodolfo, K.S., 1969. Bathymetry and marine geology of the Andaman Basin, and tectonic implications for Southeast Asia. Geol. Soc. Am. Bull. 80, 1203–1230.
Rodolfo, K.S., 1975. The Irrawaddy Delta: tertiary setting and modern offshore sedimentation. In: Broussard, M.L. (Ed.), Deltas, Models for Exploration, 2nd edn. Houston Geological Society, Houston, TX, pp. 339–356.
Rogers, K.G., Goodbred, S.L., 2010. Mass failures associated with the passage of a large tropical cyclone over the swatch of no ground submarine canyon (Bay of Bengal). Geology 38, 1051–1054. https://doi.org/10.1130/g31181.1.
Rogers, K.G., Goodbred, S.L., Khan, S.R., 2015. Shelf-to-canyon connections: Transport-related morphology and mass balance at the shallow-headed, rapidly aggrading swatch of no ground (Bay of Bengal). Mar. Geol. 369, 288–299. https://doi.org/10.1016/j.margeo.2015.09.011.
Sindhu, B., Unnikrishnan, A.S., 2013. Characteristics of tides in the Bay of Bengal. Mar. Geod. 36, 377–407.
Syvitski, J.P.M., Kettner, A.J., Overeem, I., Hutton, E.W.H., Hannon, M.T., Brakenridge, G.R., Day, J., Vorosmarty, C., Saito, Y., Giosan, L., Nicholls, R.J., 2009. Sinking deltas due to human activities. Nat. Geosci. 2, 681–686. https://doi.org/10.1038/Ngeo629.
Ta, T.K.O., Nguyen, V., Tateishi, M., Kobayashi, I., Saito, Y., 2001. Sedimentary facies, diatom and foraminifer assemblages in a late Pleistocene-Holocene incised-valley sequence from the Mekong River Delta, Bentre Province, Southern Vietnam: the BT2 core. J. Asian Earth Sci. 20, 83–94. https://doi.org/10.1016/S1367-9120(01)00028-1.
van Maren, D.S., 2007. Water and sediment dynamics in the Red River mouth and adjacent coastal zone. J. Asian Earth Sci. 29, 508–522. https://doi.org/10.1016/J.Jseaes.2006.03.012.
Walsh, J.P., Nittrouer, C.A., 2009. Understanding fine-grained river-sediment dispersal on continental margins. Mar. Geol. 263, 34–45. https://doi.org/10.1016/J.Margeo.2009.03.016.
Xu, K.H., Li, A.C., Liu, J.P., Milliman, J.D., Yang, Z.S., Liu, C.S., Kao, S.J., Wan, S.M., Xu, F.J., 2012. Provenance, structure, and formation of the mud wedge along inner continental shelf of the East China Sea: a synthesis of the Yangtze dispersal system. Mar. Geol. 291, 176–191. https://doi.org/10.1016/J.Margeo.2011.06.003.
Xue, Z., Liu, J.P., DeMaster, D., Van Nguyen, L., Ta, T.K.O., 2010. Late Holocene evolution of the Mekong Subaqueous Delta, southern Vietnam. Mar. Geol. 269, 46–60. https://doi.org/10.1016/J.Margeo.2009.12.005.